From the Klinik für Unfallchirurgie und Orthopädie

(Director: Prof. Dr. med. Andreas Seekamp)

at the University Medical Center Schleswig-Holstein, Campus Kiel

at Kiel University

Evaluation of bone allograft processing methods: Impact on decellularization efficacy, biocompatibility and mesenchymal stem cell functionality

Dissertation

to acquire the doctoral decree (Dr. med.)

at the Faculty of Medicine

at Kiel University

presented by

ALEXANDER FELIX RASCH

from Kirchheimbolanden

Kiel **2021**

1st Reviewer: Prof. Dr. rer. nat. Sabine Fuchs

2nd Reviewer: Prof. Dr. rer. nat. Jürgen Harder

Date of oral examination: 09.09.2021

Approved for printing, Kiel, 01.07.2021

Signed: Prof. Dr. rer. nat. Sabine Fuchs

(Chair of the Examination Committee)

Table of Contents

I. List of Abbreviations

Abbreviation	Full Name
ALP	Alkaline phosphatase
ANOVA	Analysis of variance
At%	Atomic percentage
BPXs	Bio-Oss processed xenografts
BSA	Bovine serum albumin
°C	Degrees Celsius
Ca/N	Calcium / nitrogen ratio
Ca/P	Calcium / phosphate ratio
CaP	Calcium phosphate
CD	Cluster of differentiation
CLSM	Confocal laser scanning microscope
cm^2	Square centimeter
CPAs	Chemically processed allografts
CPC	Cetylpyridinium chloride
CPS	Counts per second
DMEM	Dulbecco's Medium Essential Medium
DNA	Desoxyribonucleic acid
DNase	Deoxyribonuclease
dsDNA	Double stranded DNA
ECM	Extracellular matrix
EDTA	Ethylendiaminetetraacetat
EDX	Energy-dispersive x-ray spectroscopy
ePPi	Extracellular inorganic pyrophosphates
FBS	Fetal bovine serum
HIF-1	Hypoxia-inducible factor-1
HLA-DR	Human leucocyte antigen (DR isotype)
kHz	Kilohertz
kV	Kilovolt
Lsec	Live seconds
μg	Microgram
μL	Microliter

μm	Micrometer
mg	Milligram
min	Minutes
mL	Milliliter
mm	Millimeter
mM	Millimolar
MSC	Mesenchymal stem cells
MTS	3-(4,5-dimethylthiazol-2-yl)-5-(3-carboxy-methoxyphenyl)-2-(4-sulfophenyl)-2H-tetrazolium
ng	Nanogram
nm	Nanometer
no.	Number
O/Ca	Oxygen / calcium ratio
ODM	Osteogenic differentiation medium
PBS	Phosphate buffered saline
Pen/Strep	Penicillin / streptomycin
PFA	Paraformaldehyde
Pi	Inorganic phosphates
PMMA	Polymethyl methacrylate
qRT-PCR	Quantitative real-time polymerase chain reaction
SDF-1	Stromal cell-derived factor 1
SDS	Sodium dodecyl sulfate
SEM	Scanning electron microscope
SPAs	Sonication-based processed allografts
SD	Standard deviation
TNAP	Tissue non-specific alkaline phosphatase
TPAs	Tutoplast processed allografts
TRITC	Tetramethylrhodamine
U	Units
VEGF	Vascular endothelial growth factor
vs.	Versus
v/v	Volume / volume percent
w/v	Weight / volume percent
x g	Times gravity

II. Figure Index

1. Introduction

1.1 Bone grafts

According to the 3rd edition report of The Burden of Musculoskeletal Diseases in the United States, the number of people who received care after suffering bone fractures rose to more than 23 million [1]. As fracture incidences have been shown to have a bimodal distribution with a high rate for elderly people [2], an increase in fracture prevalence in an ever-aging society can be expected in the future. While most fractures heal within 3–8 weeks [3], about 5–10% of fractures end in non-unions [4], which together with infected non-unions, high-energy injuries and bone loss due to i.e. tumor resection cause critical bone defects [5]. The treatment of bone defects is challenging for the attending surgeon, and in many cases, bone grafts are required. While autologous bone grafting is currently still considered the gold standard [6,7], some limitations are associated with autologous grafting, such as risk of infections, additional surgical sites and limited bone supply [8].

Allografts and xenografts present viable alternatives to autografts as they solve the problem of limited autologous bone supply and do not require an additional surgical site for graft harvesting [9]. However, allogenic and xenogenic grafting can carry the risk of infection [10] and may induce an immunological reaction in the graft recipient [11]. Thus, a successful usage of allografts and xenografts *in vivo* requires a thorough removal of immune response eliciting material, such as bone marrow content or potential pathogens [12]. This is usually achieved by decellularizing the bone graft using a combination of chemical substances (Triton X-100, sodium dodecyl sulfate, hydrogen peroxide), enzymes (DNase, trypsin) and physical treatment (centrifugation, sonication, temperature treatment).

While decellularization may be viewed as the central step in graft processing, donor selection [13] and graft harvesting [14] have also been shown to exert an influence on the graft's properties. Properties of the bone graft such as surface area, surface structure, chemical composition and mechanical stability may be altered by the processing of the graft [15–17] and may influence the implantation *in vivo* or the growth of bone forming cells such as mesenchymal stem cells, for instance. Hence, special attention must be paid in terms of processing.

1.2 Mesenchymal stem cells

Mesenchymal stem cells (MSCs) are adult human stem cells [18] which were first described by Friedenstein et al. in the 1960s and 1970s [19]. Originally, they were isolated from bone tissue [20] and showed a multilineage potential. While MSCs account for ~ 0.01–0.001% of all cells in the bone marrow [21], they have also been successfully isolated from a variety of tissues, such as adipose tissue [22,23], peripheral blood [24], dental tissue [25], synovial fluid [26], amniotic fluid [27], Wharton's jelly [28] and from the placenta [29]. However, some authors suggest that they can be found in all organs and tissues [30].

MSCs have traditionally been described with a trilineage potential, able to differentiate into adipocytes, chondrocytes and osteoblasts. However, more recent publications describe an even greater differentiation potential of MSCs, also being able to differentiate into tendon [31], muscle [32], cardiomyocytes, pancreatic cells, hepatocytes and neuronal cells, depending on the tissue of isolation [18,33].

While the physiological functions of MSCs in situ are not yet fully comprehended, MSCs have been found to contribute to the formation of hematopoietic microenvironments, modulate the activity of immune cells and to regulate cell traffic [34].

1.2.1 Defining mesenchymal stem cells

One of the challenges presented when working with MSCs is the heterogeneous nature of MSC cultures. Different laboratories often use different isolation methods for MSCs, usually based on their ability to readily adhere to plastic. This renders MSC cultures heterogeneous, thus making it difficult to compare study outcomes conducted with MSCs across different laboratories. In order to address this problem, the International Society for Cellular Therapy published a statement in which they propose minimal criteria for the definition of mesenchymal stem cells. According to this statement, MSCs must (1) exhibit adherence to plastic, (2) display certain cell surface markers, such as CD105, CD 73 and CD90 and lack other markers such as CD45, CD34, CD14, CD19 and HLA-DR surface molecules. Additionally, (3) MSCs must show the potential to differentiate *in vitro* into adipocytes, chondrocytes and osteoblasts [35].

1.2.2 Areas of application of mesenchymal stem cells

To this date, several clinical studies have been conducted with mesenchymal stem cells which have underlined their regenerative potential in a variety of applications. A randomized, double-blinded, placebo-controlled, dose escalation study showed a significant improvement in the left ventricular ejection fractions of patients after suffering from myocardial infarction when treated with intracoronarily delivered MSCs compared to the placebo group [36]. Phase 1, 2 and 3 trials are currently ongoing for further validation of MSC treatment for cardiac regeneration [37]. Additionally, MSCs have also shown potential to support renal tissue after acute kidney infarction [38,39]. Some positive effects could be observed in patients suffering from spinal cord injury when treated with MSCs, however, what effect MSCs have on motor neuron function is still inconclusive [40]. Furthermore, MSCs also show promising results in the advancement of treatment strategies for patients with type I [41] and II [42] diabetes.
However, they have been extensively researched and used in the area of bone and cartilage repair. In patients suffering from osteoarthritis, treatment with MSCs lead to an improvement in pain and symptoms [43,44], while the generation of large sized cartilage *in vitro* has recently been accomplished using MSCs [45], creating the possibility to treat larger sized cartilage defects. Patients suffering from osteogenesis imperfecta, a genetically inherited condition resulting in brittle bones, have also profited from allogenic bone marrow transplants as the receival of new mesenchymal progenitors improved the condition [46]. Avascular femoral head osteonecrosis is another condition in which MSCs haven shown to slow progression of the disease and additionally avoid subsequent femoral head collapse and joint replacement [47,48]. Fractures resulting in atrophic non-unions, despite adequate surgical intervention have been successfully treated using autologous MSCs [49].
Likewise, MSCs show promising results concerning the treatment of critical-size bone defect [50]. *In vivo* studies have repeatedly shown an acceleration in bone repair when bone grafts were loaded with MSCs prior to implantation [51,52] and several authors have demonstrated the utility of MSCs when treating patients with atrophic bone [53,54].

1.2.3 Immunomodulatory and immune-evasive properties of mesenchymal stem cells

Another well-described characteristic of MSCs is their immunomodulatory and immuno-evasive property *in vitro*. When cultured with other cells, MSCs secrete soluble factors that have been shown to possess an immunosuppressive activity [55]. Additionally, MSCs have been shown to express no MHC class II and only low levels of MCH class I [56]. Clinical trials using allogenic MSCs have been conducted with success [36], thus raising the question if the usage of autogenic MSCs is just as effective as they have to be expanded *in vitro* 4–6 weeks prior to usage. However, more recent publications question the traditional view on immunosuppression and immuno-evasion. Several *in vivo* studies have shown a difference in study outcomes based on the usage of allogenic and autogenic MSCs [57,58]. It is proposed that this effect is observed when MSCs mature in the donor to more differentiated cells, which in turn express higher levels of MHC I and II [59], thus losing their immuno-privileged status.

The immunomodulatory properties of MSCs are also used as an explanation for study outcomes involving the treatment of diseases caused by underlying immunological issues. As such, beneficial effects of MSC treatment have been found in diseases such as Crohn's disease [60], multiple sclerosis [61], amyotrophic lateral sclerosis [62] and steroid resistant graft versus host disease [63].

1.2.4 Role of mesenchymal stem cells in bone formation

Mesenchymal stem cells also play a pivotal role during bone formation after bone fractures. After a fracture, blood vessels rupture and a hematoma is formed, preventing further loss of blood and of bioactive factors [64]. Initial fracture site environment is characterized by inflammation and hypoxia, promoting and signaling immune cells participating in the healing process [65] and bone progenitors are recruited to the site of fracture around day 3 [66]. While this migration to the fracture site is not yet completely understood and several factors are involved, [67] the stromal cell-derived factor 1 (SDF-1)/CXCL12 CXCR4 chemotactic axis is the most researched mechanism in this context [68,69]. Inhibition of this pathway significantly alters fracture repair [70]. MSCs migrate to the fracture site from several niches such as the periosteum, endosteum, bone marrow [71] and the perivascular niche [72]. The occurrence of

MSCs in the perivascular niche is not limited to bone tissue but mesenchymal stem cells have been shown to be present in the perivascular niche throughout the entire body [73]. This might explain why authors establish that MSCs have been found in various organs such as the spleen, kidney, liver, lungs, pancreas, brain, aorta and the vena cava [30,74]. Circulating MSCs have also been found, however, it is not clear yet to what extent they are recruited in fracture healing [75,76]. After the fracture hematoma has formed, SDF-1 levels rise [77], which in turn attracts CXCR4 expressing cells. Since the SDF-1 gene is regulated by the hypoxia-inducible factor-1 (HIF-1) [78], hypoxia in the fracture hematoma contributes to chemotactic factor secretion and cell migration. Additionally, the hypoxic environment induces the secretion of vascular endothelial growth factor (VEGF) [79], stimulating the formation of new blood vessels which is critical for new bone formation [80]. MSCs have shown to significantly contribute to VEGF secretion [81]. Following migration, MSCs differentiate into osteogenic cells and contribute to the formation of bone substance [82].

1.2.5 Osteogenic differentiation of mesenchymal stem cells

Osteogenic differentiation of MSCs is a two-step process: (1) lineage commitment and (2) maturation [83]. The process of lineage commitment is complex, controlled by multiple factors. Ascorbic acid has been found to increase extracellular matrix (ECM) secretion followed by an upregulation of osteogenic markers such as alkaline phosphatase (ALP) and osteocalcin [84]. Dexamethasone, on the other hand, increased cell proliferation and ALP activity [85] while β-glycerophosphate provides phosphates for mineral deposition [84]. Countless chemical factors are involved in osteogenic differentiation, which may act in a synergistical fashion [86]. In addition to chemical factors, physical factors such as mechanical forces [87] and biological factors such as oxygen supply have also shown to influence differentiation. Hypoxia is known to inhibit osteogenic differentiation [88] and to promote MSC to differentiate into cartilage [89], thus underlining the importance of vascularization in bone repair. The process of osteogenic maturation is usually evaluated using histochemical and molecular biological methods. The expression of osteogenic genes such as osteopontin, osteonectin, osteocalcin, bone morphogenic protein 2 (BMP-2) and alkaline phosphatase can be evaluated using quantitative real-time polymerase chain

reaction (qRT-PCR) [90]. Additionally, ALP activity can be quantified by using an alkaline phosphatase assay. Following maturation, MSCs start to deposit calcium (Ca^{2+}), which is also referred to as the mineralization phase [91]. These calcium depositions can be stained with Alizarin Red and evaluated either histologically or quantified photocolorimetrically [92].

1.2.6 Alkaline phosphatase

Alkaline phosphatase is an enzyme found on the outer cell membrane of many different cells in the body and exists in different isotypes [93]. The prevalent form found in bone tissue is the tissue non-specific alkaline phosphatase (TNAP). While the importance of ALP activity in mineralization has been thoroughly established, its exact mechanism is not yet completely understood. ALP is transcribed early in the process of osteogenic differentiation, rising ~ 11 days after osteogenic induction and decreasing during the phase of early mineralization [91]. This points, at least in part, to a role in the early phase of mineralization. Early cues on its role and function were derived from patients suffering from mutations in the ALP gene. In these patients, severe forms of hypophosphatasia could be observed [94]. These findings led to the understanding that ALP uses extracellular inorganic pyrophosphates (ePPi) as a substrate and hydrolyzes them to inorganic phosphate (Pi), which is a mineralization promoter [95]. Thus, ALP provides phosphates for the synthesis of hydroxyapatite, a mineral that makes up bone substance and in which calcium and phosphates are stored [96], as well as reducing inhibitors for mineralization (ePPi) [95].

1.3 Mesenchymal stem cell applications in conjunction with bone grafts

MSCs have also been studied in depth in conjunction with evaluating bone grafts. Bone grafts have shown the potential to influence differentiation of MSCs into the osteogenic lineage [97,98]. Furthermore, the combined application of MSCs and bone grafts demonstrated enhanced healing properties of large bone defects *in vivo* after implantation [99,100]. However, only a few studies have been conducted that investigate the usage of bone grafts loaded with stem cells for the treatment of bone defects in human subjects [101–103]. This might be in part due to the efforts involved

in harvesting and expanding autologous MSCs and the small number of patients with bone defects for whom standard treatment procedures are unsuitable.

In addition to their ability to produce new bone tissue, the therapeutic potential of MSCs has in part been attributed to paracrine effects that MSCs exert via cytokines and growth factors [104] on adjacent MSCs and bone tissue upon integration *in vivo* [105]. At the same time, cytokine secretion by MSCs and bone forming cells can be influenced by the implant's properties, such as in CaP containing grafts, being able to influence the cells' secretome towards an osteogenic profile through adenosine signaling [106]. Physicochemical properties of the graft have a direct influence on cell adherence and cell proliferation of MSCs after seeding onto bone grafts [107–109], playing an important role upon application of seeded grafts *in vivo*. Ideally, the processing of bone grafts for tissue engineering applications should decellularize the graft completely, inactivate any potential harmful pathogens, maintain biomechanical stability and in conjunction with stem cell applications, demonstrate osteoconductive or osteoinductive properties combined with high biocompatibility as defined by Williams [110].

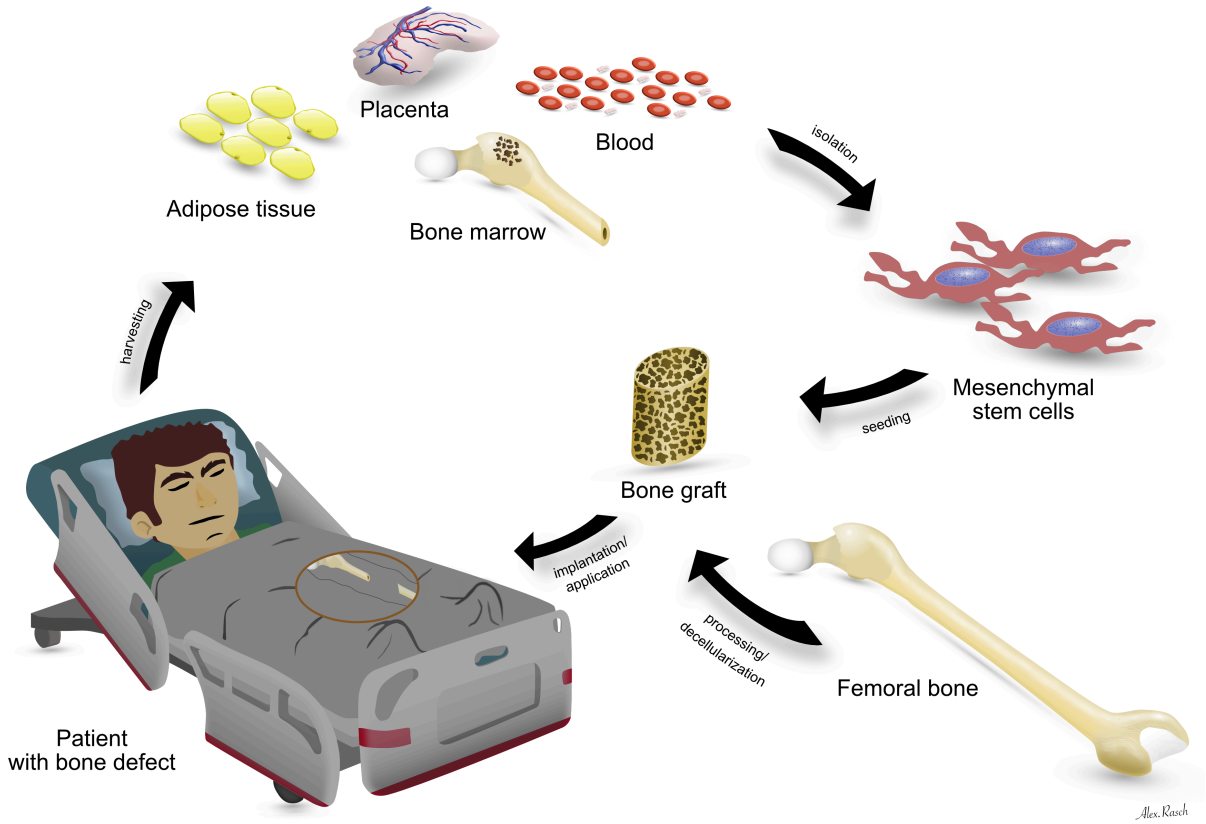

Figure 1. Overview - Mesenchymal stem cell therapy in patients with bone defects. Bone grafts are regularly used when treating patients with bone defects. These bone grafts can be harvested and processed from xenogenic or allogenic bone sources without the necessity to create an

additional surgical site. Mesenchymal stem cells on the other hand can be isolated from various tissues such as adipose tissue, bone marrow, blood and the placenta and have shown the potential to support healing processes. Recent studies have also shown MSCs to improve graft integration and bone regeneration when seeded onto bone grafts prior to implantation. Hence, this work focuses on the processing of bone grafts and their *in vitro* ability to host MSCs, allow for adequate proliferation and osteo-induce seeded MSCs.

1.4 Aim and objectives

Several decellularization methods, such as decellularization based on chemical treatment [111], sonication [112] and irradiation [113] have been proposed, yet it remains unclear which method results in favorable properties for *in vivo* use as well as favorable reseeding properties in conjunction with MSCs. In this study, we compare two decellularization methods adapted from published protocols for bone grafts based on chemical treatment [111] or sonication [112]. The effect of each method on the graft's surface texture, composition and decellularization, including bone marrow removal, was investigated. Decellularized grafts as well as two commercially available grafts, one allograft (Tutoplast®) and one xenograft (Bio-Oss®), were further subjected to element analysis and MSC viability assays with extracts derived from the grafts. Commercially available grafts were included in this study as additional references for standardized graft processing. Self-decellularized grafts as well as commercially available grafts were reseeded with MSCs pre-differentiated in osteogenic medium and cell adhesion, proliferation and osteogenic activity was assessed in order to compare their performance in conjunction with MSCs.

2. Materials and Methods

2.1 Ethical approval

The use of human tissue and cells was approved by the local ethical advisory board of the Medical Faculty of Christian-Albrechts-University in Kiel (Approval number - D459/13), Germany, including the consent from the individual donors.

2.2 Comparison of two decellularization approaches

2.2.1 Cutting and preparation of bone cylinders

Femoral heads were obtained from patients undergoing total hip replacement surgery due to coxarthrosis. Criteria for exclusion was necrosis, tumor and infections. Donors consisted of five female and five male donors, ranging in age from 42 to 93 years (mean 73.2 years, SD ± 18.9 years) and 51 to 80 years (mean 69.8 years, SD ± 14.5 years), respectively.

Upon receival, femoral heads were placed in tissue buffer, consisting of GlutaMAX™ Medium 199 (Gibco, Darmstadt, Germany), 15% (v/v) fetal bovine serum (FBS) (Sigma, Taufkirchen, Germany), 1% (v/v) (100 U/mL / 100 µg/mL) Penicillin/Streptomycin (Pen/Strep) (Biochrom, Berlin, Germany), 1% (v/v) (20 µg/mL) Ciprofloxacin (Fresenius Kabi, Bad Homburg, Germany), 1% (v/v) (2.5 µg/mL) Amphotericin B (Biozol, Eching, Germany) and were then cut into slices using a table saw (Proxxon, Wecker, Luxembourg). This was done in conjunction with custom-built additions to the table saw. (1) A metal slider to the right of the saw blade served as protection (see Figure 2). (2) A custom-built slider with a metal right angle mounted on top, which could be adjusted in the direction of the x-axis and the y-axis, served as a stabilizer. Femoral heads were cut into discs with a thickness of 5 mm. For this, a caliper (Steinle, Ingelfingen, Germany) was used to adjust the distance between the saw blade and the cut guide in order to obtain bone discs with the proper thickness. After disinfecting all instruments and devices used for bone cutting with 70% (v/v) ethanol (Merck, Darmstadt, Germany) and additionally with Biocidal (WAK Chemie Medical, Steinbach, Germany), the femoral head was cut along the cut guide in a circular movement with a bone holding forceps (Aesculap, Tuttlingen, Germany). This was performed under aseptic conditions with the use of sterile surgical gloves (CardinalHealth, Dublin, OH, USA).

Once the bone discs were cut, cylinders with a 6 mm diameter were cut out of the bone discs with a trephine hollow drill (Hager & Meisinger, Neuss, Germany) and a laser guided bench drilling machine (Bosch, Stuttgart, Germany) (Figure 3). Prior to decellularization, bone cylinders were washed in tissue buffer, placed in 48-well plates and stored at -80°C without the addition of buffers or liquids.

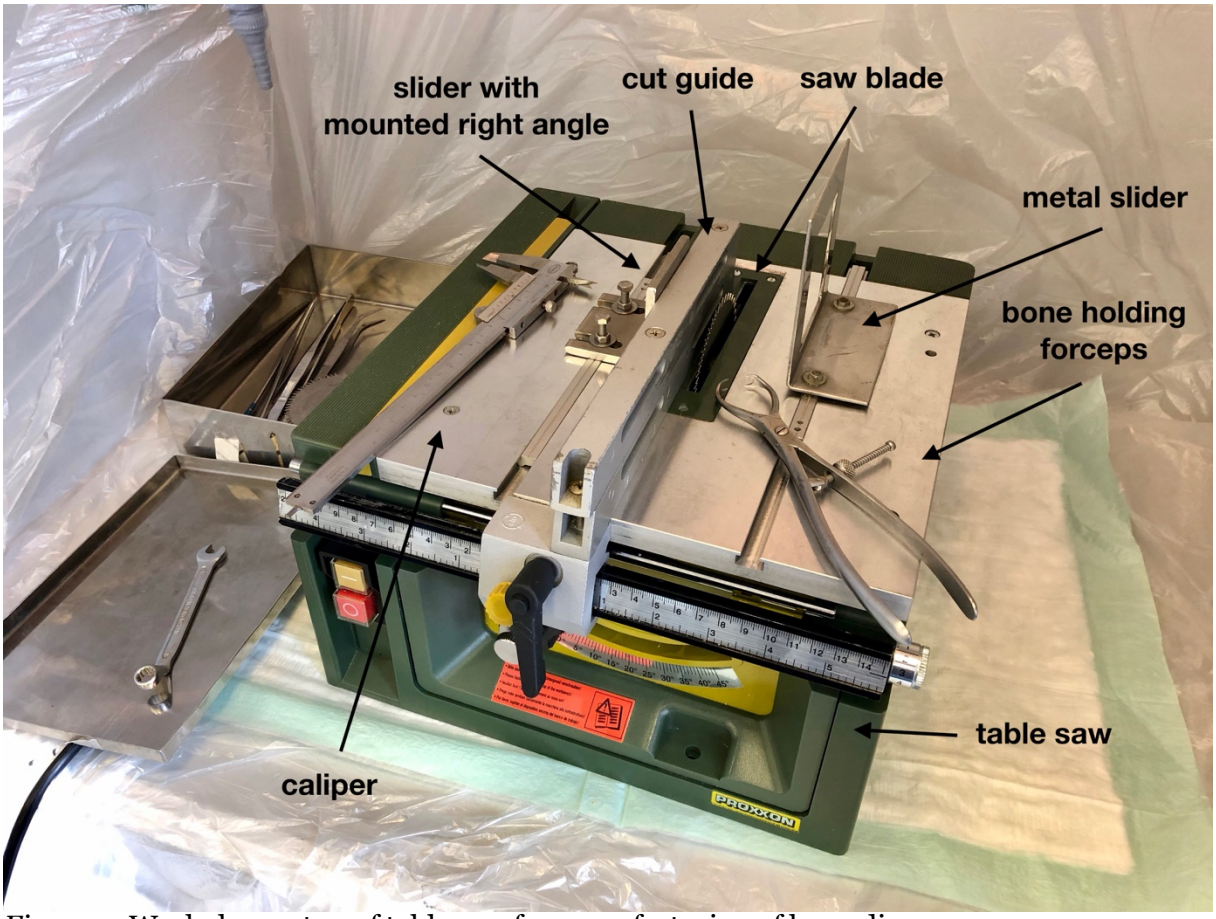

Figure 2. Workplace setup of table saw for manufacturing of bone discs.

Figure 3. Workplace setup of laser guided bench drilling machine for manufacturing of bone cylinders.

2.2.2 Decellularization of allografts based on chemical treatment

After defrosting, chemical decellularization was initiated by 3 freeze/thaw cycles with liquid nitrogen. For this, liquid nitrogen was poured into a container and bone cylinders were submerged using forceps (Aesculap, Tuttlingen, Germany) and a holding tube (Th. Geyer, Renningen, Germany). This was followed by placing the bone grafts in a 48-well plate and incubating them two times for 24 hours, each in 750 µL 2% (v/v) Triton X-100 (Sigma-Aldrich, Taufkirchen, Germany) diluted with phosphate-buffered saline (PBS) (Fisher Scientific, Loughborough, UK). All solutions were sterile filtered before use. Incubation of bone grafts for decellularization purposes was always performed at room temperature on an orbital shaker (Edmung Bühler, Bodelshausen, Germany) if not otherwise specified. After treatment with Triton X-100, bone grafts were incubated for 24 hours in 750 µL 1% (w/v) sodium dodecyl sulfate (SDS) (Sigma-Aldrich, Darmstadt, Germany) solution diluted in PBS. Then, they were washed with PBS for 30 min on an orbital shaker and incubated with 200 U/mL DNase I (Sigma-Aldrich, Darmstadt, Germany) solution at 37°C for 12 hours using a dry block incubator (Eppendorf, Hamburg, Germany). The procedure was finished by washing the allografts three times for 2 hours with PBS on an orbital shaker. Allografts decellularized by this protocol are henceforth referred to as chemically processed allografts (CPAs).

2.2.3 Decellularization of allografts based on sonication

Grafts decellularized using sonication are referred to as sonication-based processed allografts (SPAs). Bone grafts were defrosted from -80°C, submerged in 1 mL of distilled water preheated to 60°C and sonicated for 15 min at 20 kHz with an amplitude of 12 microns using a sonication needle (Mk2 sonicator, MSE, London, UK). Allografts were then rinsed with PBS until the solution became clear and were then placed in 750 µL PBS on an orbital shaker for 2 hours at 60°C. This was succeeded by a wash-centrifuge sequence repeated three times. The sequence consisted in a washing step with distilled water at 60°C on an orbital shaker and a centrifugation step at 1850 x g for 15 min at room temperature (Heraeus, Hanau, Germany). The first washing step was performed for 30 min while the second and third for 10 min. Allografts were then sonicated first in 1 mL 3% (v/v) hydrogen peroxide (Sigma-Aldrich, Darmstadt, Germany) solution diluted with PBS at 60°C, and then in 1 mL 70% (v/v) ethanol (Th.

Geyer, Renningen, Germany) diluted with distilled water at room temperature, both for 10 min at 20 kHz and with an amplitude of 12 microns. Allografts were then placed in distilled water at 60°C for 10 min on an orbital shaker and centrifuged for 15 min at 1850 x g at room temperature. Decellularization was finished by placing allografts in distilled water at room temperature for 30 min on an orbital shaker. After completion of either CPA or SPA protocol, allografts were thoroughly washed and stored without the addition of buffers or solutions at 4°C until use.

2.2.4 Commercial allografts and xenografts

Tutoplast® (RTI Surgical, Alachua, FL, USA) and Bio-Oss® (Geistlich, Wolhusen, Switzerland) grafts were acquired as cancellous bone blocks from human and bovine origin, respectively, and were cut into cylinders with the same dimensions as used for decellularization. This was performed using a drilling machine (Dremel, Mt. Prospect, USA) with a 6 mm trephine hollow drill. As the cancellous bone blocks measured 1 cm in height, the cylinders were cut in half using a scalpel (Feather, Osaka, Japan) and a caliper to obtain the same size of the decellularized bone cylinders (6 mm diameter, 5 mm height) as mentioned above. This process was performed under sterile conditions with a laminar flow workbench using sterile surgical gloves and sterile instruments. The drilling machine and the hollow drill were disinfected with both 70% (v/v) ethanol and Biocidal before use. Bio-Oss® and Tutoplast® are hence forth referred to as Bio-Oss® processed xenografts (BPXs) and Tutoplast® processed allografts (TPAs).

2.2.5 Histological examination of decellularized allografts

Histological examination was performed by fixation of bone cylinders in 4% paraformaldehyde (PFA) (Morphisto, Frankfurt am Main, Germany) for 24 hours. Samples were embedded in polymethyl methacrylate (PMMA) using a tissue processor (Tissue Processor TPC 15, Medite, Burgdorf, Germany). The medium in which the samples were embedded (PMMA) consisted of 500 g methyl methacrylate (MMA) (Fluka, Neu-Ulm, Germany), 3 g 2,2′-Azobis(2-methylpropionitrile) (Merck, Darmstadt, Germany), 100 mL Nonylphenol-polyethylene glycol acetate (Walter-CMP, Kiel, Germany) and 5 mL phthalic acid butyl ester (Merck, Darmstadt, Germany). After each sample was embedded and completely hardened in a 37°C water bath, they were cut using a bandsaw (Metabo, Nürtingen, Germany) and then polished with a grinding

machine (DP-U4, Struers, Erkrath, Germany) from 500-grit sandpaper to a 4000-grit paper. Once the samples were polished to a high gloss polish, they were glued onto a plastic microscope slide and the sample was horizontally cut along the slide with a thickness of approximately 200 μm using a high precision bandsaw (Exakt, Norderstedt, Germany). The thickness of the sample was further reduced to 40-60 μm using a high precision grinding machine (Exakt, Norderstedt, Germany) and microscope slides with samples were then polished to a high gloss polish.
Staining was performed by consecutively incubating slides for 2 min with 0.1% (v/v) formic acid (Merck, Darmstadt, Germany), 90 min in 20% (v/v) methanol (Merck, Darmstadt, Germany) and 2 min in toluidine blue staining solution (Merck, Darmstadt, Germany). Solutions were diluted in distilled water, and in-between each step, slides were washed in distilled water. Images were taken with EVOS FL Auto 2 Imaging System (ThermoFisher Scientific, Bothell USA).

2.2.6 Analysis via scanning electron microscopy

Specimens were prepared for scanning electron microscopy (SEM) by fixation in 3% (v/v) glutaraldehyde (Sigma-Aldrich, Darmstadt, Germany) diluted in PBS. Following fixation for 24 hours, samples were treated with ethanol gradients ranging from 50% up to 99% (v/v) ethanol. For this, ethanol solutions with 50%, 60%, 70%, 80%, 90%, 96% and 99% (v/v) ethanol were prepared. Specimens were consecutively incubated with each concentration for 2-5 min and then placed on specimen-tables (Agar Scientific, Stansted, UK) using carbon adhesive discs (Agar Scientific, Stansted, UK). Prior to imaging 3 µL of hexamethyldisilazane (ThermoFisher, Kandel, Germany) were applied and samples were gold sputtered with a 10 nm thick layer (SCD 005 Cool Sputter Coater, Bal-Tec, Balzers, Lichtenstein). Images were taken with Philips XL 30 CP SEM (Philips, Amsterdam, Netherlands).

2.2.7 DNA quantification of decellularized allografts

In order to assess the degree of decellularization, DNA content was quantified from CPAs, SPAs, TPAs and BPXs. Additionally, controls that had not been treated other than by storing at -80°C were analyzed as a reference. Grafts were placed in 2 mL Eppendorf tubes and 1 mL nuclease-free water (Ambion, Carlsbad, CA, USA) was added. Then, three freeze/thaw cycles at -80°C and sonication for 30 seconds at 20

kHz and with an amplitude of 12 microns using a sonication needle was performed. After centrifuging at 2000 x g for 5 min at room temperature, the supernatant was transferred, and the total DNA amount quantified with Quant-iT PicoGreen® dsDNA assay kit (Molecular probes, Eugene, OR, USA). According to the assay kit manual standard DNA solutions were prepared with concentrations ranging from 1 ng/mL to 2000 ng/mL DNA. After placing 100 μL of buffer solution to each well on a 96-well plate (Greiner Bio-One, Kremsmünser, Austria) 28 μL of standard solutions and samples solutions were added to the corresponding wells. Then, 72 μL of PicoGreen® solution was added which is an ultrasensitive fluorescent nucleic acid stain for quantitating double stranded DNA (dsDNA) as it emits fluorescent light when attached to dsDNA and excited by 485 nm light. Using standard DNA solutions, a standard curve was created from which DNA amount of sample values were calculated. Sample solutions were diluted appropriately to fit inside the standard curve.

DNA quantification for each bone graft material (CPAs, SPAs, TPAs and BPXs) was performed for two cylinders from 3 donors in technical triplicates. The DNA amount was quantified as mentioned above by fluorescence with a microplate reader (TECAN, Maennedorf, Switzerland) at an excitation wavelength of 485 nm and an emission wavelength of 535 nm.

2.2.8 Energy-dispersive X-ray spectroscopy

Energy-dispersive x-ray spectroscopy (EDX) analysis was performed using a Philips XL 30 CP SEM. Prior to analysis, samples were sputtered with carbon. The SEM was operated with 25 kV and examined areas on grafts were chosen so that 2100 counts per second (CPS) were registered and dead time was 30–35%. Measurements were performed for a period of 200 live seconds (Lsec). Three donors were used for each bone graft material. Each cylinder was measured twice at two different surface areas of the graft.

2.3 Comparison of reseeding properties with MSCs

2.3.1 Isolation and culture of MSCs

MSCs were isolated from cancellous bone of the femoral heads obtained from patients undergoing total hip replacement surgery. Isolation was performed as previously

mentioned [114,115]. Femoral heads were received from patients undergoing total hip replacement surgery. Upon receival, femoral heads had been pre-cut in the operating room into quarters and were placed in tissue buffer preheated to 37°C. Working with sterile surgical gloves, pieces of cancellous bone were collected from the bone with a Luer forceps (Aesculap, Tuttlingen, Germany). Cancellous bone fragments were collected in Falcon 50mL tubes and PBS was added. After thoroughly shaking the tube, PBS was transferred to a new tube and the process was repeated until approximately 6-8 Falcon tubes with PBS washing solution were obtained. Tubes with PBS wash solution were then centrifuged at 400 x g for 10 min. After the supernatant was aspirated the cell pallet on the bottom of the tube was reconstituted with 5 mL buffy coat buffer, consisting of PBS, 0.5% (v/v) FBS and 2 mM Ethylendiaminetetraacetat (EDTA) (SERVA, Heidelberg, Germany). Resuspended cells were then collected and run through a 40 μm cell strainer (Falcon, Durham, USA) and counted using an automated cell counter (CASY TT, OLS, Bremen, Germany). Cells were seeded in T175 flasks coated with collagen type I (Corning, Bedford, MA, USA) at a density of $2x10^6$ cells/cm^2 and incubated at 37°C in Dulbecco's Medium Essential Medium (DMEM)/Ham's F-12 medium (Biochrom, Berlin, Germany) supplemented with 20% (v/v) FBS and 1% (v/v) Pen/Strep for the first 14 days. The first medium change was performed 24 hours after seeding to remove cells that had not attached to the flask. Henceforth, the medium was changed three times a week. After splitting cells from passage 0 to passage 1, culturing was continued using 10% (v/v) FBS. In passage 2 osteogenic differentiation of MSCs was induced by incubation in osteogenic differentiation medium (ODM) for a minimum of two weeks consisting of DMEM/Ham's F-12, 10% (v/v) FBS, 1% (v/v) Pen/Strep, 10 mM β-glycerophosphate (Sigma-Aldrich, Darmstadt, Germany), 0.1 µM dexamethasone (Sigma-Aldrich, Darmstadt, Germany) and 50 µM ascorbic acid (Sigma-Aldrich, Darmstadt, Germany). Experiments with MSCs were conducted with cells in passage no. 4 and 5.

2.3.2 Biocompatibility testing using extracts obtained from decellularized bone grafts

In order to assess the biocompatibility of decellularized grafts, extracts of CPAs, SPAs, TPAs and BPXs were prepared according to ISO 10993. Then, the effect of extracts on MSC viability was assessed using MTS (3-(4,5-dimethylthiazol-2-yl)-5-(3-

carboxymethoxyphenyl)-2-(4-sulfophenyl)-2H-tetrazolium). Extracts were created by incubating decellularized bone grafts in 750 µL ODM at 37°C for either 24 hours or 72 hours and stored at -20°C until use. MSCs were seeded at a density of 45,500 cells/cm^2 in a 96 well-plate (Sarstedt, Nümbrecht, Germany) that had been pre-coated with 33.6 µg/mL collagen type I solution diluted in PBS. After allowing cells to attach for 24 hours, ODM was aspirated, extracts were defrosted, centrifuged at 12,000 x g for 5 min, added to the cells and incubated for 48 hours. Metabolic activity of MSCs was assessed using CellTiter 96® AQueous One Solution Cell Proliferation Assay (Promega, Madison, WI, USA) according to manufacturer's instructions. The MTS compound is a reagent that can be bioreduced by cells into a colored product and is presumed to be accomplished by dehydrogenase enzymes in metabolically active cells. Thus, the metabolic activity can be quantified colorimetrically. After incubating the cells with the extracts for 48 hours the extract solution was aspirated, and 100 μL of MTS reagent solution and 20 μL of ODM was added to the wells. After 2 hours of incubation the optical density was measured with a microplate reader (TECAN, Maennedorf, Switzerland) at 490 nm. Three MSC donors and three distinct bone donors for CPAs and SPAs were used to assess biocompatibility in technical triplicates. Data were depicted in relation to untreated controls.

2.3.3 Seeding of MSCs onto constructs

After coating grafts with 10 µg/mL fibronectin (Millipore, Temecula, CA, USA) 200,000 MSCs were drop seeded in a volume of 100 µL ODM onto precoated CPAs, SPAs, TPAs and BPXs, placed in 48-well plate wells. After cells were left to attach to grafts for 1 hour at 37°C 650 µL of ODM was added and medium was exchanged three times a week.

2.3.4 Evaluation of MSC-seeded constructs by CLSM and SEM microscopy

After 7 days of cultivation, MSC-seeded constructs were fixed in 4% PFA solution followed by three wash cycles in PBS for 15 min and twice for 5 min. Samples were then treated with 0.5% (v/v) Triton X-100 diluted in PBS for 20 min. This was followed by washing in PBS. Intracellular F-actin was stained with 5 µg/mL tetramethylrhodamine (TRITC)-conjugated phalloidin (Sigma-Aldrich, Darmstadt,

Germany) in 1% (v/v) bovine serum albumin (BSA) (Millipore, Kankakee, USA) in PBS for 30 min. Hoechst 33258 (Sigma-Aldrich, Darmstadt, Germany) at a concentration of 2 µg/mL in PBS for 15 min was used for nuclear counterstain. Samples were imaged by confocal laser scanning microscope (CLSM) (LSM 510 Meta, Zeiss, Oberkochen, Germany). After CLSM, MSC-seeded constructs were prepared for SEM as described above.

2.3.5 DNA quantification of MSC-seeded constructs

In order to evaluate cell attachment and cell proliferation of MSCs on SPAs, TPAs and BPXs, DNA quantification was performed on day 1, day 7 and day 14 after cell seeding. MSC-seeded constructs were transferred into new 48 well-plate wells and DNA was extracted by performing three freeze/thaw cycles at -80°C after the addition of nuclease-free water, followed by sonication at a frequency of 20 kHz and an amplitude of 12 microns for 30 seconds. At each time point DNA quantification was performed for two independent grafts and technical replicates for 3 donors. DNA quantification was performed as described above.

2.3.6 ALP assay

ALP activity was measured from supernatants of MSC-seeded constructs after day one, day seven and day fourteen using an alkaline phosphatase assay kit (Abcam, Cambridge, UK). Measurements were run in technical triplicates and ALP activity measurements were performed according to manufacturer's instructions. Based on this kit, an ALP enzyme solution serves as a standard from which a standard curve is calculated. P-nitrophenyl phosphate (*p*NPP) is used as a substrate that can be dephosphorylated by ALP to p-Nitrophenol (*p*NP) and measured photocolorimetrically at OD 405 nm as a result of its change in color. ALP activity (in U/mL) was calculated as follows: $\left(\frac{B}{\Delta T\ x\ V}\right) * D$, where B equals the amount of *p*NP in sample well calculated from the standard curve (*µ*mol), ΔT equals the reaction time (in minutes), V equals the original sample volume added into the reaction well (mL) and D equals the dilution factor. Measurements were normalized to 1 µg DNA at the indicated time points. At each time point, ALP quantification was performed for two independent grafts and technical replicates for 3 donors.

2.3.7 Alizarin Red S quantification

Alizarin Red S staining was performed to assess mineralization of MSCs on SPAs, TPAs and BPXs. After 7 and 14 days of cultivation, MSC-seeded constructs were fixed in 4% PFA for 1 hour in a 48-well plate, washed three times with PBS and consecutively incubated in 500 µL Alizarin Red S staining solution (40 mM, Merck, Darmstadt, Germany) for 60 min at room temperature on an orbital shaker. After washing MSC-seeded constructs with distilled water in order to remove any excess, Alizarin Red S was extracted using a 10% (w/v) cetylpyridinium chloride (CPC) solution (Carl Roth, Karlsruhe, Germany) for 48 hours in a new 48-well plate. Finally, extracted Alizarin Red S was quantified by measuring the optical density at 560 nm and calculated in accordance with the standard curve. At each time point, Alizarin Red S quantification was performed for two independent grafts and technical replicates for 3 donors.

2.4 Statistical analysis

Statistical analysis was carried out using GraphPad Prism 7. Statistical significance was assessed using ANOVA, as indicated in the individual experiments. A p-value of $p < 0.05$ (* $p < 0.05$, ** $p < 0.01$, *** $p < 0.001$, **** $p < 0.0001$) was considered to be statistically significant.

3. Results

3.1 Comparison of two decellularization approaches

3.1.1 Histological examination of decellularized allografts

Histological examination of decellularized bone grafts with toluidine blue staining was performed in order to assess the decellularization efficacy of chemical and sonication-based decellularization protocols (Figure 4). Untreated controls (Figure 4A) show trabecular structures in blue and marrow cavities extensively filled with bone marrow. Higher magnification of this sample (Figure 4B) shows deposited matrix peripherally to the trabecular structures (white arrow). Furthermore, cells showing the morphology of adipocytes can be detected in the marrow cavity (thin black arrow). CPAs only contain little to no marrow content (Figure 4C). However, some trabecular fragments in the

marrow cavities (thick black arrow) can be seen (Figure 4D). SPAs show completely empty marrow cavities and very distinct trabecular structures (Figure 4E). Higher magnification (Figure 4F) confirms marrow cavities void of any material.

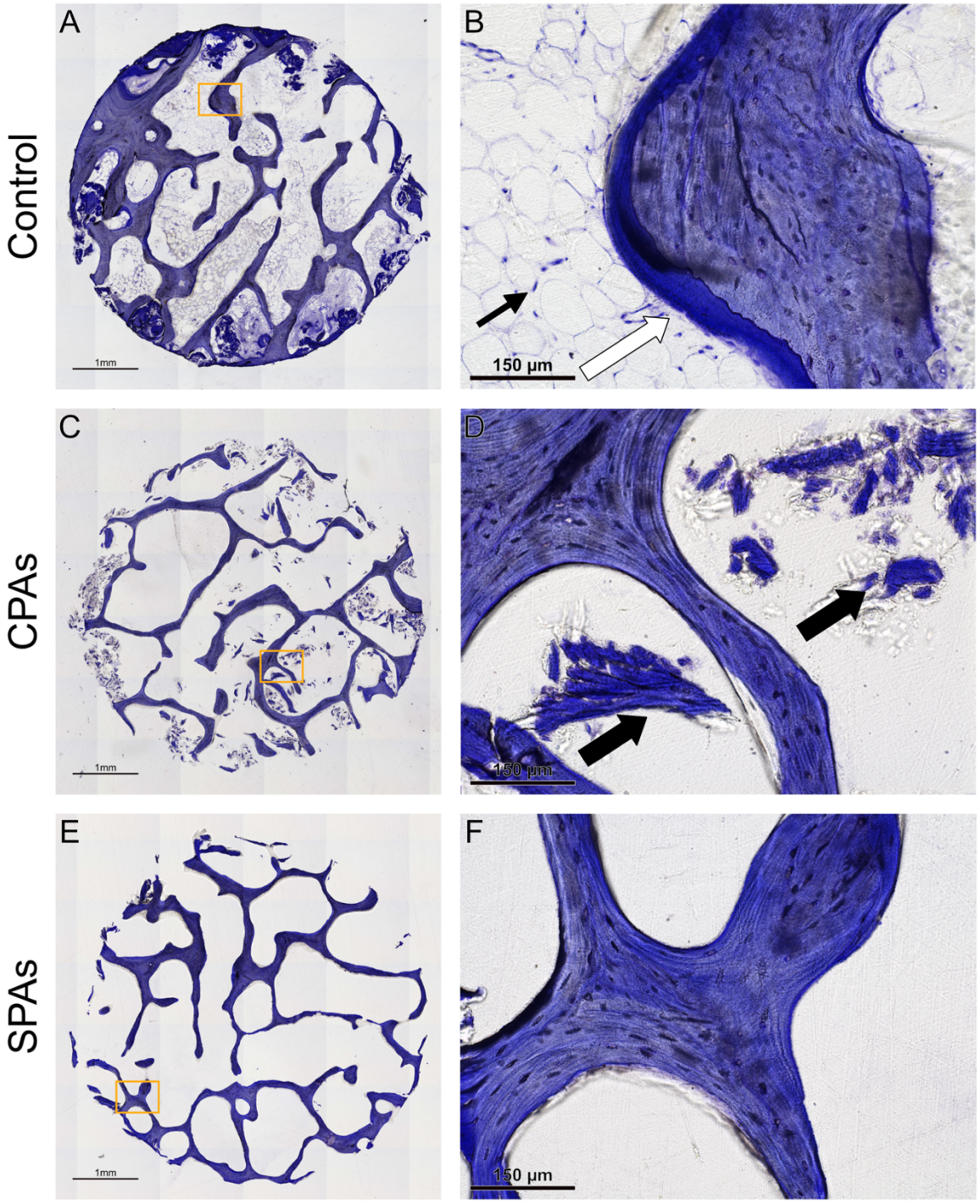

Figure 4. Histological assessment of chemically processed allografts, sonication-based processed allografts and controls. Toluidine blue stained sections show untreated control allografts (A, B), chemically processed allografts (C, D) and sonication-based processed allografts (E, F). Images document less cells and residues of bone marrow in sonication-based processed allografts compared to chemically processed allografts and control. White arrow (B) points to deposited matrix, thin black arrow (B) to peripherally located nuclei of adipocytes

and black thick arrows (D) point to trabecular fragments. Images A, C, E show stitched images using 42 individual images. Scale bar: A, C, E = 1 mm, B, D, F = 150 µm.

3.1.2 SEM images of decellularized allografts

In order to confirm histological examination and to further assess the surface topography of decellularized bone grafts, SEM images were taken (Figure 5). SEM images of untreated controls (Figure 5A) display a similar surface structure compared to CPAs (Figure 5C). Surface structure of SPAs (Figure 5E) differs visually from controls and CPAs. Additionally, SPAs (Figure 5F) display more trabecular structures devoid of bone marrow or soft tissue in the cavities compared to CPAs (Figure 5D). CPAs show a surface topography that resembles those of untreated control grafts (Figure 5B).

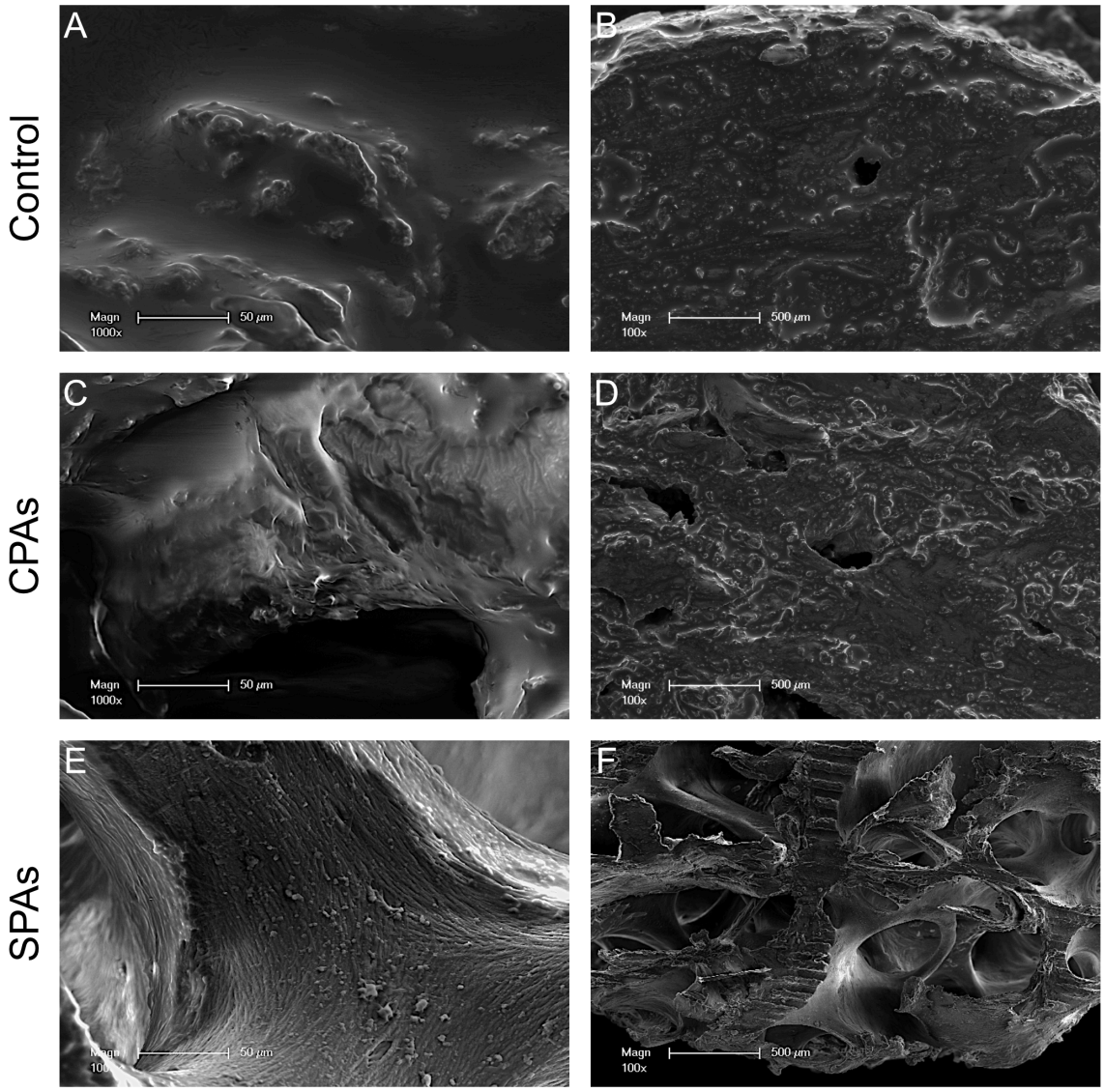

Figure 5. Scanning electron microscope assessment of chemically processed allografts, sonication-based processed allografts and controls. Scanning electron microscope images show untreated control allografts (A, B), chemically processed allografts (C, D) and sonication-

based processed allografts (E, F). Scanning electron microscope images depict more empty marrow cavities for sonication-based processed allografts in comparison to chemically processed allografts and control. Scale bar: A, C, E = 50 μm, B, D, F = 500 μm.

3.1.3 DNA quantification of decellularized allografts

In order to further verify and assess the efficacy of the decellularization protocols for CPAs and SPAs, DNA was quantified. Furthermore, as additional references and controls, DNA contents of commercially available and standardized grafts (TPAs and BPXs) were measured (Figure 6). DNA is depicted as absolute values (Figure 6A) and in relation to control allografts that had not been decellularized (Figure 6B). Decellularized CPAs revealed a mean value of 15,304 ng DNA. SPAs yielded a mean value of 40.3 ng, while controls showed an average of 58,279 ng. TPAs and BPXs yielded a total amount of 7.4 ng and 0.49 ng DNA, respectively. In relation to untreated controls, CPAs showed a non-significant DNA reduction to 85.98%, while SPAs showed a significant DNA reduction to 0.11%. Compared to controls, DNA levels of TPAs and BPXs showed a significant DNA reduction to 0.01% and 0%, respectively. These data suggest a much more effective decellularization for the SPA compared to CPA processed grafts. Decellularization efficacy for SPA was tentatively lower but still comparable to the two commercially available grafts used as additional references.

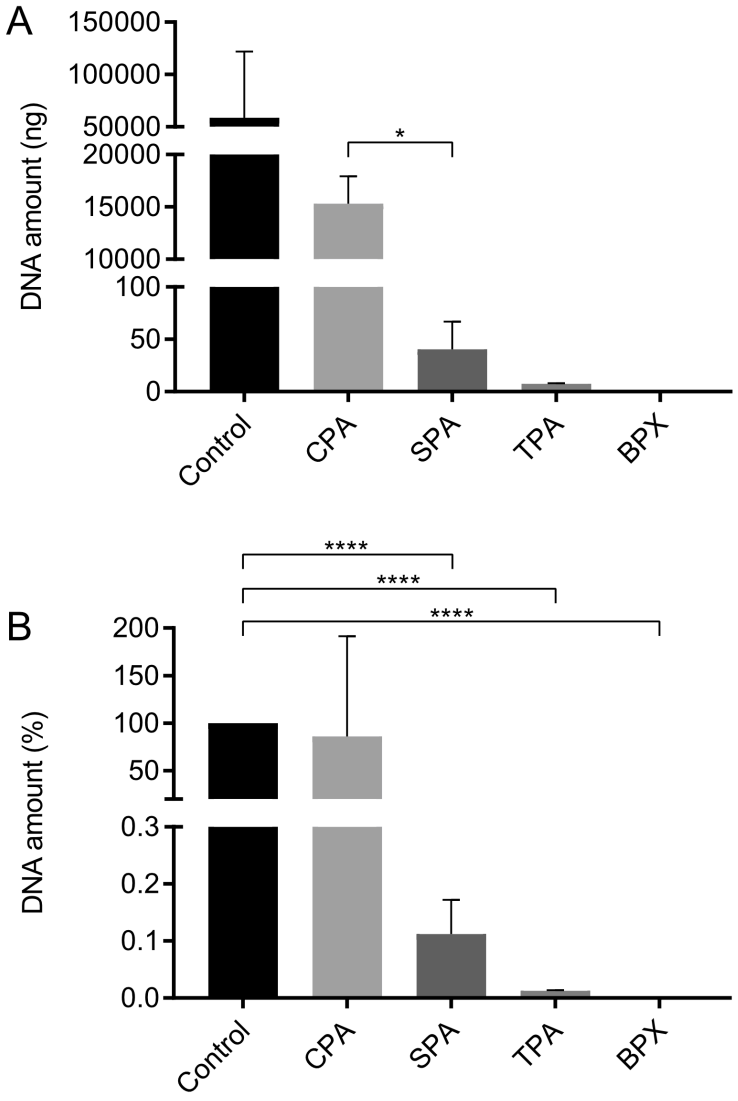

Figure 6. DNA quantification of chemically processed allografts, sonication-based processed allografts, and commercially available allografts (Tutoplast processed allografts) and xenografts (Bio-Oss processed xenografts). Highest amounts of residual DNA were detected in chemically processed allografts which differed significantly from SPAs, based on Tukey's multiple comparison in conjunction with ANOVA. TPAs and BPXs show low amounts of DNA (A). Values of sonication-based processed allografts, TPAs and BPXs are significantly lower compared to control (B), as assessed by Tukey's multiple comparison in conjunction with ANOVA (n = 3 donors, two independent grafts were measured per donor, * $p < 0.05$, **** $p < 0.0001$).

3.1.4 EDX analysis

Element analysis was performed by EDX spectroscopy to reveal the elemental composition of CPAs and SPAs and compare it to commercially available TPAs and BPXs. Figure 7A shows significant differences in atomic percentage (At%) between CPAs and SPAs for oxygen (O) (12.88%) and nitrogen (N) (-10.06%). Among all bone grafts, TPAs displayed the least amount of calcium (Ca) and phosphorous (P) and the highest amount of N, differing significantly from all other tested grafts. BPXs showed the highest values in Ca and P, including significant differences to CPAs and TPAs with regard to Ca and significant differences to TPAs with regard to P. Values for N in BPXs were low, showing significant differences to SPAs and TPAs. Since it has previously been shown that grafts with a Ca/P ratio of ~ 1.43 can induce osteogenesis [106], Ca/P ratios were displayed (Figure 7B). In addition, Ca/N and O/Ca ratios were displayed as N and O are ubiquitous in many organic compounds. For the bone essential Ca/P ratios did not differ significantly between grafts. However, TPAs showed the lowest Ca/N ratio whereas the O/Ca ratio was highest, showing significant differences compared to all other grafts.

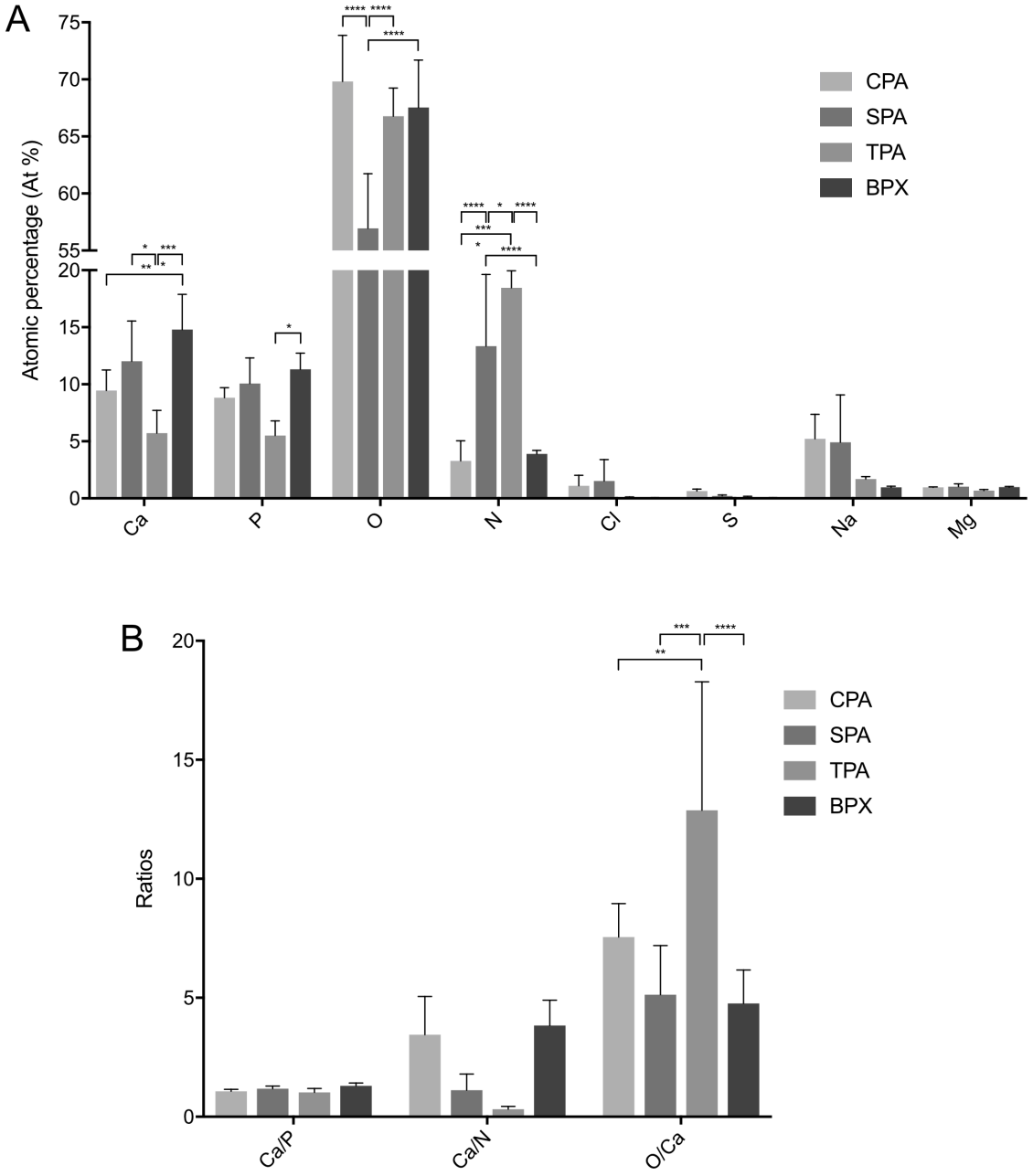

Figure 7. Energy-dispersive x-ray spectroscopy analysis of chemically processed allografts, sonication-based processed allografts, Tutoplast processed allografts and Bio-Oss processed xenografts. Analysis shows element composition in atomic percentage (At%) (A) and Ca/P, Ca/N and O/Ca ratios (B) in order to assess chemical composition. Tutoplast processed allografts show the highest amount of N, a low Ca/N ratio and high O/Ca ratio while Bio-Oss processed xenografts show the highest values for Ca and P. Statistics are based on Tukey's multiple comparison in conjunction with ANOVA (n = 3 donors, two different surface areas were measured per donor,* $p < 0.05$,** $p < 0.01$,*** $p < 0.001$,**** $p < 0.0001$).

3.2 Comparison of reseeding properties with MSCs

3.2.1 Biocompatibility testing using extracts obtained from decellularized bone grafts

In order to assess potentially harmful substances leaking out of the processed bone grafts, extracts were created by adding ODM to CPAs, SPAs, TPAs and BPXs and biocompatibility was assessed by MTS assay using MSCs. Extracts were created by incubating allografts and xenografts in ODM for 24 hours and 72 hours and were then added to MSCs on 96 well-plates 24 hours after seeding. After 48 hours of exposure to extracts, MTS assay was performed. Images of seeded MSCs were taken 24h hours after treatment using EVOS microscope in translucent mode.

3.2.1.1 Testing of grafts with in-between freezing

SPAs and CPAs used for biocompatibility testing were processed and decellularized as described above. Initially, SPAs and CPAs were frozen in -80°C after decellularization for practical reasons. Results of MTS assay (Figure 8A) performed after 48 hours of exposure to the extracts (extraction time 24 hours) showed an average of 1.84% of cell viability for CPAs, while cell viability for SPAs was 15.93%. BPXs, which were commercially acquired and had not been frozen, showed an average amount of 47.61%. Corresponding microscope images (Figure 8B), taken 48 hours after exposure to extracts of CPAs, SPAs and BPXs, depict low cell densities for all grafts, while cells treated with extracts from BPXs show the largest cell size and CPAs the smallest cell size. Additionally, cells treated with extracts from CPAs displayed a roundish, dysmorphic morphology.

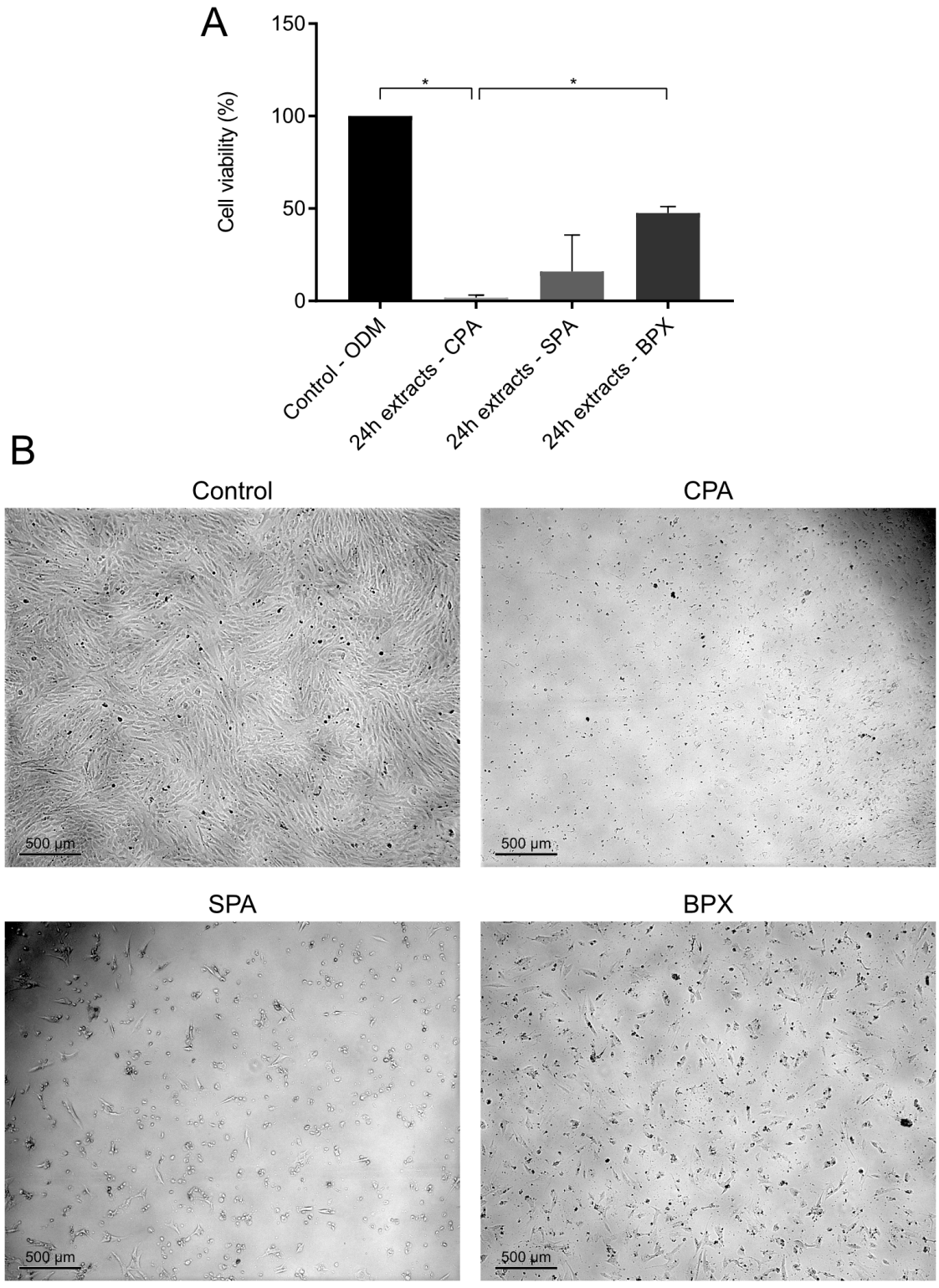

Figure 8. Biocompatibility testing with mesenchymal stem cells performed for extracts of chemically processed allografts and sonication-based processed allografts in-between frozen and Bio-Oss processed xenografts. Allografts and xenografts, *which had been stored at -80°C in-between,* were incubated in osteogenic differentiation medium for 24 hours to create extracts. Extracts were then added to mesenchymal stem cells on 96 well-plates after cell attached to wells for 24 hours. After 48 hours of exposure to extracts MTS assay was performed (A). Chemically processed and sonication-based processed allografts show poor levels of cell viability after treatment with extracts. Cell viability of chemically processed allografts differed

significantly from control. Corresponding images taken 48 hours after exposure to extracts show a similar pattern (B). Statistics are based on Tukey's multiple comparison in conjunction with ANOVA (n = 2 donors, measurements were performed in technical triplicates, * $p < 0.05$).

3.2.1.2 Testing of grafts with in-between freezing and centrifugation of extracts

Since initial biocompatibility testing, described above, showed poor results for CPAs and SPAs, a proposal was made to see whether centrifuging extracts prior to usage would increase the cell viability. As such, extracts of CPAs, SPAs and also BPXs were centrifuged at 12,000 x g for 5 min prior to incubation with MSCs. However, as seen in Figure 8, cell viability for CPAs and SPAs still stayed below 2% for 24-hour extracts (Figure 9A) and 72-hour extracts (Figure 9B). Cell viability of BPXs stayed at 44.45%. Cells in corresponding images (Figure 9C) taken 48 hours after exposure to extracts appear to show a similar morphology and cell density as images in previous figure (Figure 8B).

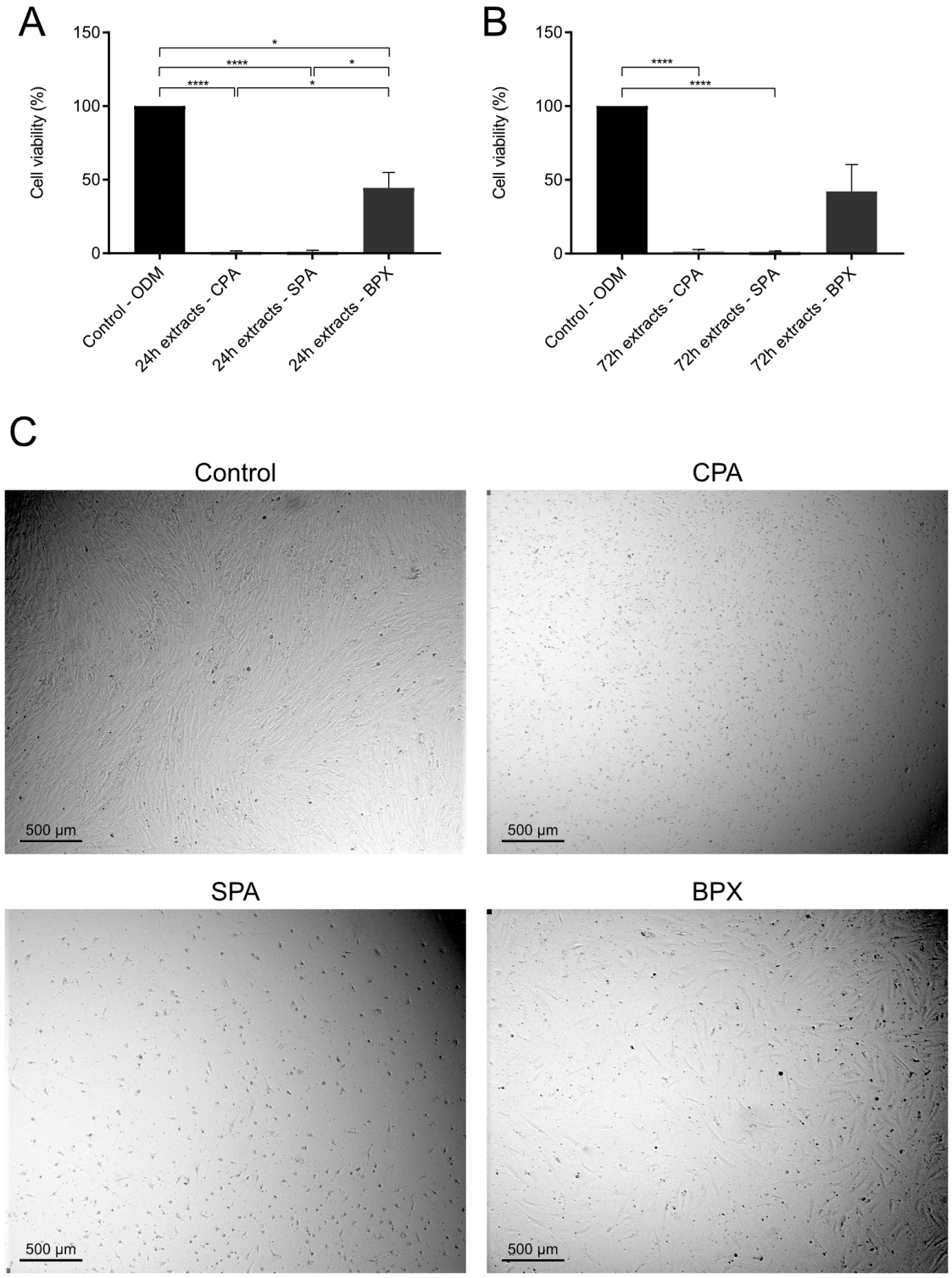

Figure 9. Biocompatibility testing with mesenchymal stem cells performed for extracts of chemically processed allografts and sonication-based processed allografts in-between frozen and centrifuged and Bio-Oss processed xenografts centrifuged. Allografts and xenografts, *which had been stored at -80°C in-between,* were incubated in osteogenic differentiation medium for 24 hours (A) or 72 hours (B) to create extracts. *After centrifugation at 12,000 x g for 5 min* extracts were added to mesenchymal stem cells on 96 well-plates after cell attached to wells for 24 hours. After 48 hours of exposure to extracts, MTS assay was performed. Chemically processed allografts and sonication-based processed allografts show poor levels of

cell viability after treatment with extracts. Cell viability of chemically processed allografts differed significantly from control. Corresponding images taken 48 hours after exposure to extracts show a similar pattern (C). Statistics are based on Tukey's multiple comparison in conjunction with ANOVA (n = 3 donors, measurements were performed in technical triplicates, * $p < 0.05$, **** $p < 0.0001$).

3.2.1.3. Testing of grafts with in-between freezing and sterile filtering of extracts

As the causing agent for the reduction in cell viability could not be removed using centrifugation, a proposal was made to sterile filter the extracts prior to the addition of MSCs. This was accomplished by using a 0.2 μm filter (Sarstedt, Nümbrecht, Germany) through which the extracts were passed prior to incubation with MSCs. Figure 10 displays microscopy images of cells 48 hours after treatment. MSCs treated with ODM as control showed a high cell density with an elongated cell morphology. Cells treated with extracts from CPAs showed a low cell density with a mostly roundish morphology. Cell morphology in images of cells treated with extracts obtained from SPAs was similar to CPAs, yet cell density appeared to be higher.

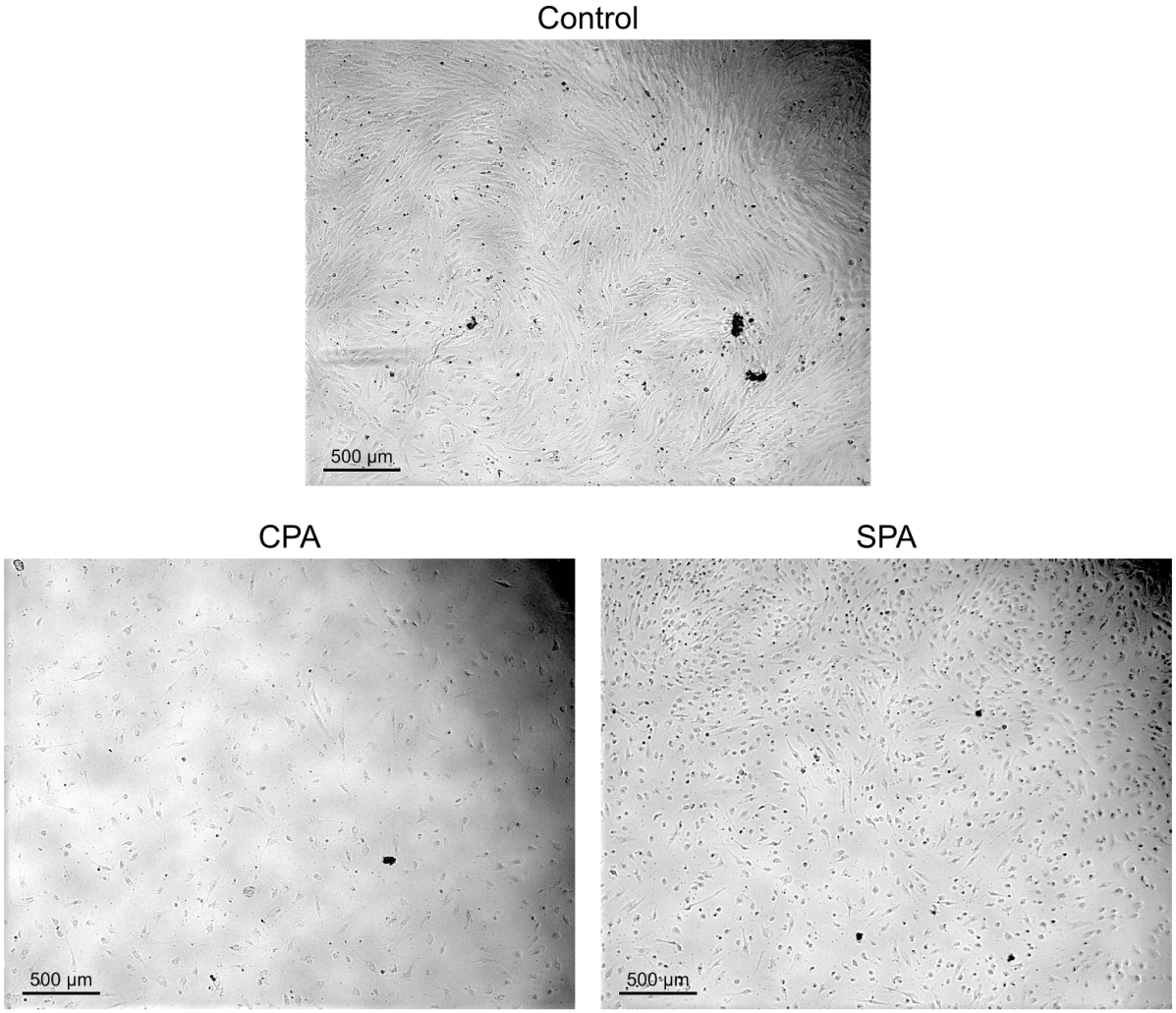

Figure 10. Biocompatibility testing with mesenchymal stem cells performed for extracts of chemically processed allografts and sonication-based processed allografts in-between frozen and sterile filtered. Allografts *which had been stored at -80°C in-between,* were incubated in osteogenic differentiation medium for 24 hours to create extracts. *After sterile filtration with a 0.2 µm filter,* extracts were added to mesenchymal stem cells on 96 well-plates after cell attached to wells for 24 hours. After 48 hours of exposure to extracts, microscopy images were recorded. Mesenchymal stem cells treated with osteogenic differentiation medium as control showed a high cell density with an elongated cell morphology. In contrast to the control, cells treated with extracts from chemically processed allografts and sonication-based processed allografts still showed a low cell density and a roundish, dysmorphic cell morphology.

3.2.1.4 Testing of grafts without in-between freezing and centrifugation of extracts

Up to this point, neither centrifuging extracts at 12 000 x g for 5 min nor sterile filtering them before adding them to MSCs showed any significant improvement of MSC viability.

Initially, CPAs and SPAs were stored at -80°C as decellularization according to the decellularization protocols for CPAs and SPAs as described above was completed. This was done so that experiments could be started for both grafts at the same time as the decellularization process endured different time lengths and to preserve the grafts in their decellularized status. As none of the above-mentioned methods resolved the issue of low biocompatibility of the extracts based on MSC cell viability, the proposal was made that the in-between freezing of the allografts for storage until usage could potentially liberate apoptosis inducing agents. Thus, CPAs and SPAs were not frozen at -80°C after decellularization for storage but were rather store at 4°C until usage and extract were additionally centrifuged at 12,000 x g for 5 min. Results of MTS assay using 24-hour extracts showed a cell viability for CPA extracts of 62.04%, for SPA extracts 51.17% and BPX extracts 36.94% (Figure 11A). TPA extracts were additionally added to biocompatibility testing and in contrast to all other grafts showed a non-significant increase (112.28%). Extracts gained by 72-hour extraction time showed similar results (Figure 11B). Accordingly, the highest values in cell viability were observed for TPAs. In conjunction with the increased cell viability in CPAs and SPAs microscopy images (Figure 11C) taken after treatment with extracts showed a change in morphology in comparison to previous trials from a roundish, dysmorphic to an elongated spindle-like cell morphology. However, compared to controls, cell density was still lower.

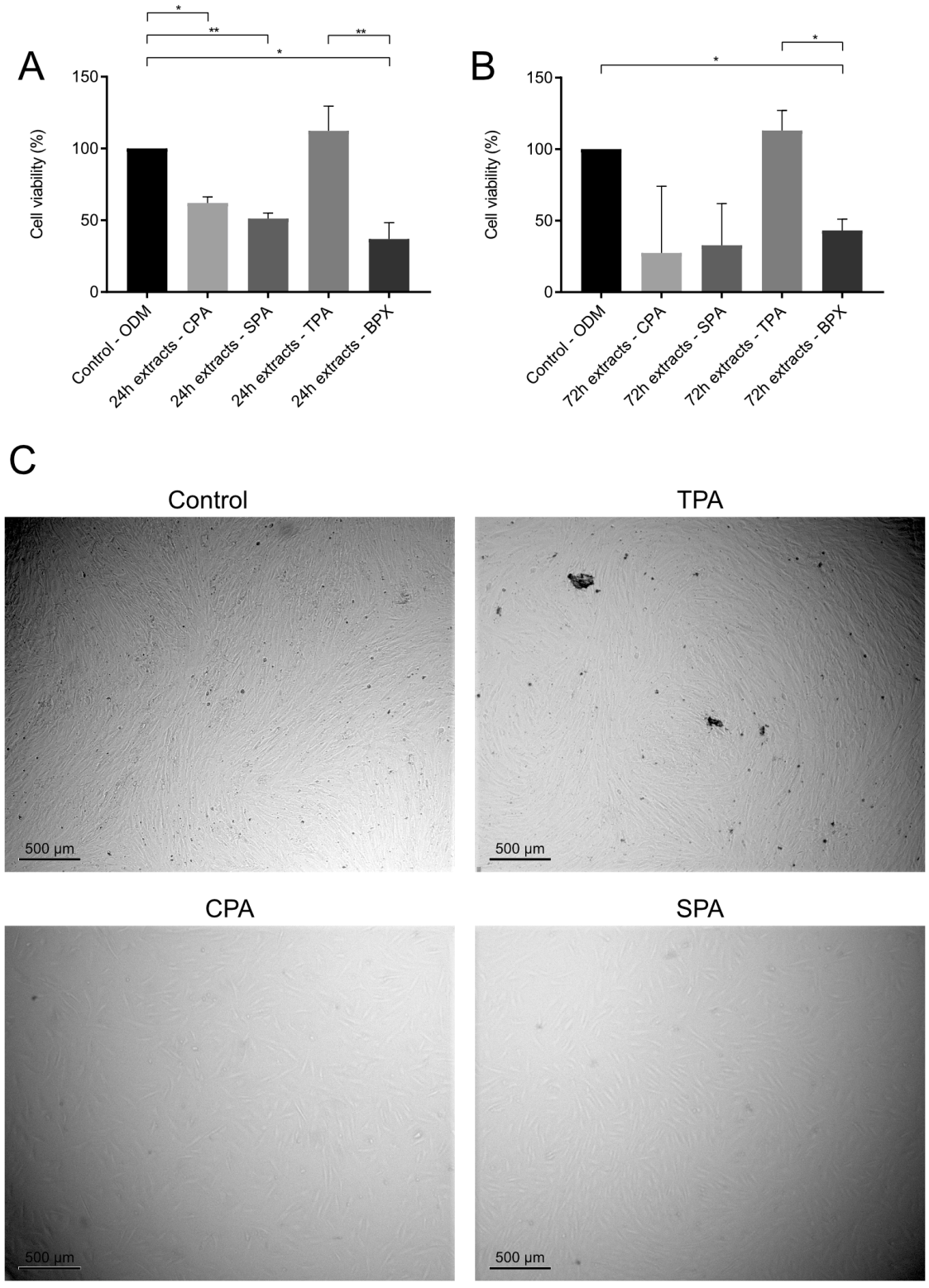

Figure 11. Biocompatibility testing with mesenchymal stem cells performed for extracts of chemically processed allografts and sonication-based processed allografts *not* in-between frozen and Tutoplast processed allografts and Bio-Oss processed xenografts. Allografts and xenografts, *which had been stored at 4°C in-between,* were incubated in osteogenic differentiation medium for 24 hours (A) or 72 hours (B) to create extracts. *After centrifugation at 12,000 x g for 5 min* extracts were added to mesenchymal stem cells on 96 well-plates after cell attached to wells for 24 hours. After 48 hours of exposure to extracts MTS assay was performed. Chemically processed allografts and sonication-based processed allografts now

show levels of cell viability similar to Bio-Oss processed xenografts (A and B). In comparison to all other grafts, Tutoplast processed allografts showed no reduction in cell viability. Corresponding images taken 48 hours after exposure to extracts now show an elongated, spindle-like morphology of mesenchymal stem cells treated with extracts from chemically processed allografts and sonication-based processed allografts (C). Statistics are based on Tukey's multiple comparison in conjunction with ANOVA (n = 3 donors, measurements were performed in technical triplicates, * $p < 0.05$, ** $p < 0.01$).

Comparing the treatment groups with 24-hour extracts (Figure 12) previously described, a significant increase in cell viability could be observed between extracts of CPAs and SPAs which had been created after grafts were stored at -80°C after decellularization vs. grafts that were stored at 4°C. Extract that had been created from grafts stored at -80°C and had additionally been centrifuged prior to addition to cells did not show any increase in cell viability. Extracts obtained from BPXs did not show any significant increase in cell viability when extracts were centrifuged.

As extracts obtained from CPAs and SPAs by storing at 4°C showed a significant increase in cell viability in-between storage at -80°C was abandoned and for all experiments in conjunction with MSCs grafts were henceforth stored at 4°C until use.

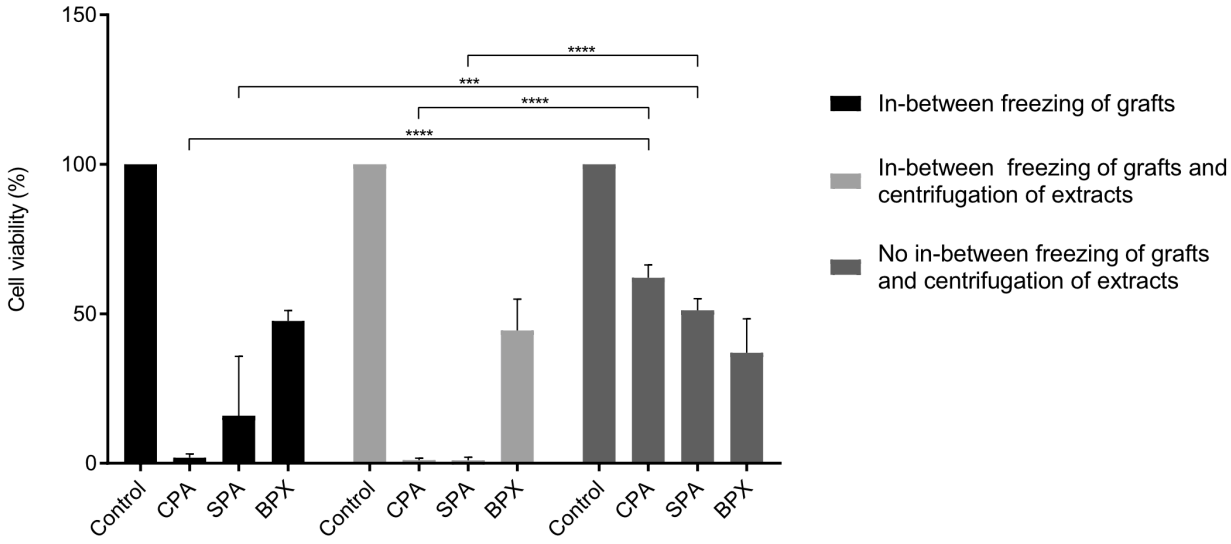

Figure 12. Biocompatibility testing performed with mesenchymal stem cells for 24-hour extracts of chemically processed allografts, sonication-based processed allografts and Bio-Oss processed xenografts using different protocols. Displayed are 3 different treatment groups of grafts. First, chemically processed allografts and sonication-based processed allografts were stored at -80°C after decellularization. Extracts were added directly to mesenchymal stem cells. Second, all extracts were centrifuged at 12,000 x g for 5 min prior to addition to mesenchymal stem cells. Third, chemically processed allografts and sonication-based processed allografts were not stored at -80°C but were kept at 4°C until use. These extracts were also centrifuged.

MTS assay was performed after cells were incubated with extracts for 48 hours. Statistics are based on Tukey's multiple comparison in conjunction with ANOVA (n = 2 donors black bars, n = 3 donors grey bars, measurements were performed in technical triplicates, *** $p < 0.001$, **** $p < 0.0001$).

3.2.2 Evaluation of MSC-seeded constructs by CLSM and SEM microscopy

While previous results characterized SPAs and CPAs after the decellularization, the following results were obtained after these grafts were reseeded with MSCs. First, CLSM images of cell- seeded constructs were taken 7 days after seeding (Figure 13). F-Actin staining was used to visualize the cytoskeleton and cells were depicted in combination with nuclear counterstain. Images of cell-seeded CPAs (Figure 13A and 13B) display some background fluorescence in the red channel due to the material properties interfering to some extent with a distinct fluorescence pattern for the cytoskeleton. Nevertheless, several nuclei are visible, confirming the presence of cells on CPAs. Images of cell-seeded SPAs (Figure 13C) show abundant numbers of MSCs revealing an elongated morphology with centrally located nuclei (Figure 13D). CLSM images of cell-seeded TPAs (Figure 13E) show a high cell density. Upon higher magnification (Figure 13F), cells seem to display a smaller morphology than cells on SPAs (Figure 13D). MSCs on BPXs (Figure 13G and 13H) show cellular protrusions with a morphology not as elongated compared to SPAs and TPAs. Additionally, the cell density appears to be lower than on MSC-seeded SPAs and TPAs.

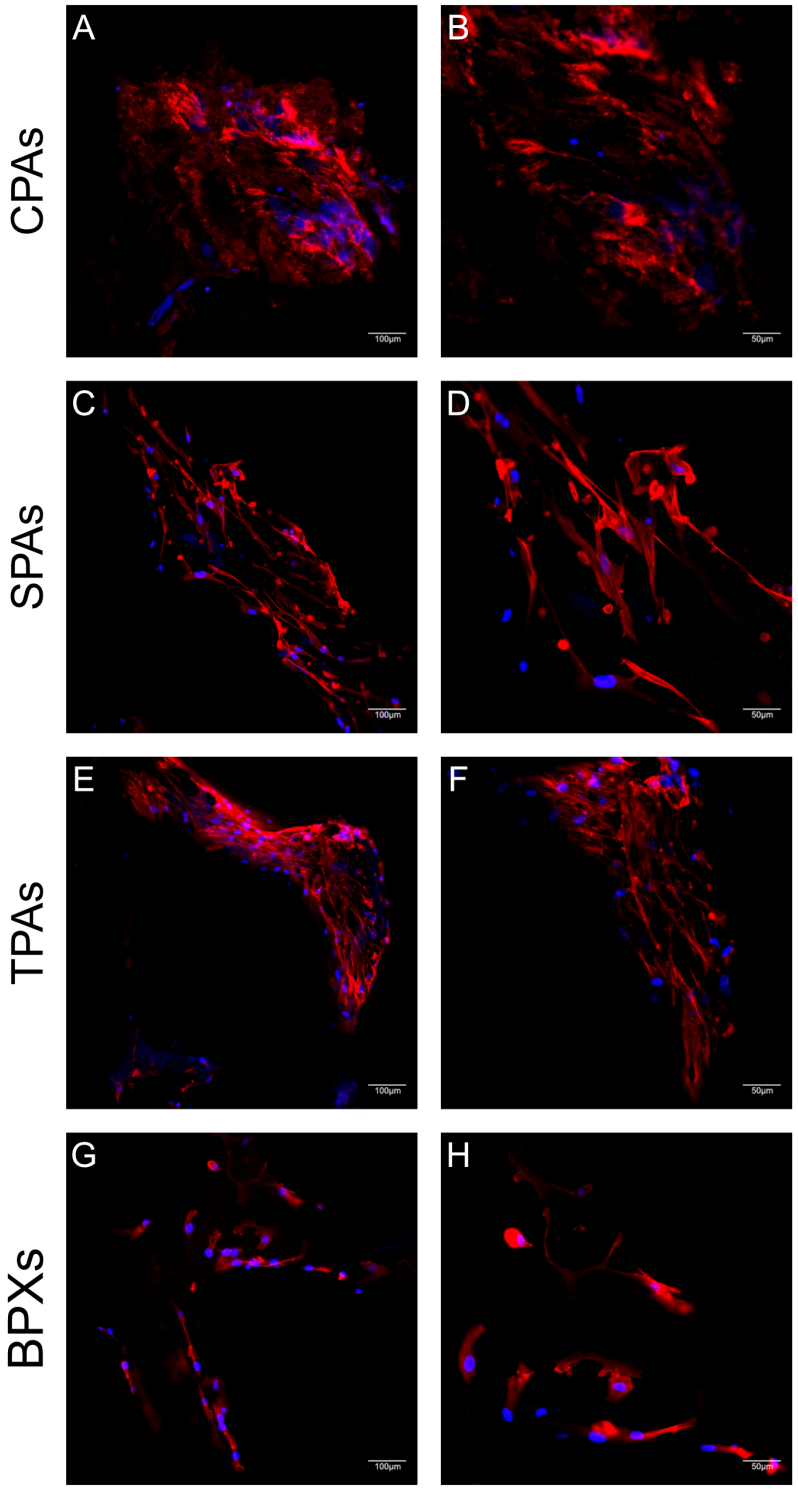

Figure 13. Morphology assessment of seeded mesenchymal stem cells on chemically processed allografts, sonication-based processed allografts, Tutoplast processed allografts and Bio-Oss processed xenografts using confocal laser scanning microscopy. Images display mesenchymal 7 days after seeding onto chemically processed allografts (A, B), sonication-based processed allografts (C, D), Tutoplast processed allografts (E, F) and Bio-Oss processed xenografts (G, H) stained with TRITC-conjugated phalloidin / Hoechst nuclear stain co-stain. Images of chemically processed allografts depict cells, but as well, high levels of background fluorescence. mesenchymal stem cells on Bio-Oss processed xenografts show a lower cell density than cells on sonication-based processed allografts and Tutoplast processed allografts. Scale bars: A, C, E, G = 100 µm, B, D, F, H = 50 µm.

SEM images of MSC-seeded constructs shown in Figure 14 reflect findings from CLSM images. Cell-seeded CPAs (Figure 14A and 14B) display elongated cells and nuclear protrusions (white arrows). MSC-seeded SPAs also show elongated cells with several nuclear protrusions (Figure 14C and 14D). Congruent to CLSM images, MSCs on TPAs (Figure 14E) display a smaller morphology with a high number of cellular processes (Figure 14F). Seeded BPXs (Figure 14G and 14H) show few cells with few elongated processes analogous to Figure 13H.

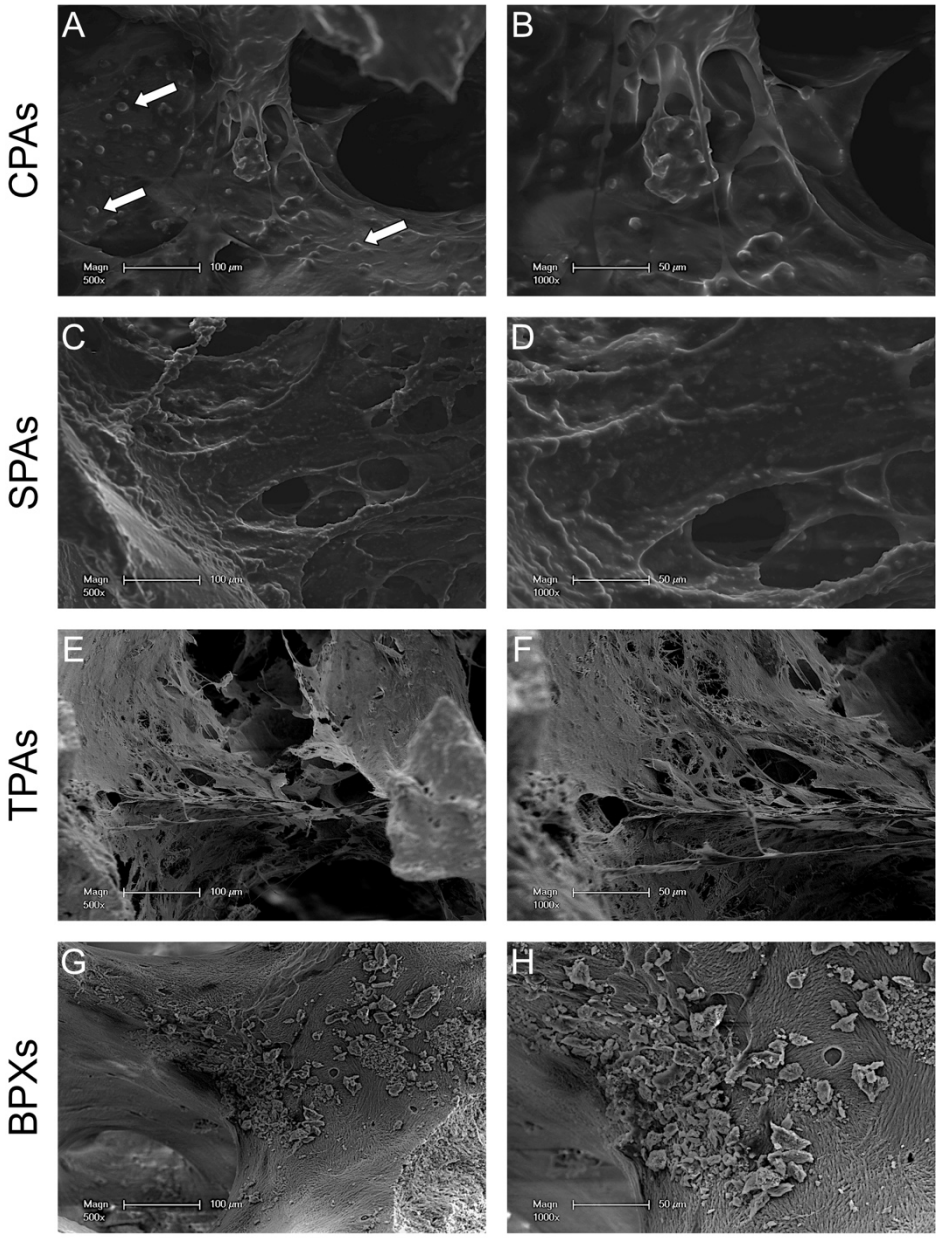

Figure 14. Morphology assessment of seeded mesenchymal stem cells on chemically processed allografts, sonication-based processed allografts, Tutoplast processed allografts and Bio-Oss processed xenografts using scanning electron microscopy. Images show mesenchymal stem cells 7 days after seeding onto chemically processed allografts, (A, B), sonication-based processed allografts (C, D), Tutoplast processed allografts (E, F) and Bio-Oss processed

xenografts (G, H). Chemically processed allografts, sonication-based processed allografts and Tutoplast processed allografts show elongated spindle-like cells while mesenchymal stem cells on Bio-Oss processed xenografts appear to be fewer in number. White arrows point to nuclear protrusions. Scale bars: A, C, E, G = 100 µm, B, D, F, H = 50 µm.

3.2.3 DNA quantification of MSC-seeded constructs

Cell adhesion to grafts (day 1) as well as the rate of proliferation (day 7 and 14) of MSCs on SPAs, TPAs and BPXs was determined by DNA quantification (Figure 15). The DNA content of corresponding unseeded grafts was subtracted as background for each group. In consequence to the results from Figure 6 where CPAs did not reveal a sufficient level of decellularization, CPA data were excluded from quantitative evaluation of the MSC performance after reseeding.

DNA quantification after reseeding showed a significant increase of MSC numbers grown on TPAs on day 14 (2077 ng) compared to day 1 (685.7 ng) and day 7 (864.5 ng), thus indicating the proliferation of MSCs on TPAs in the investigated time frame. In addition, after 14 days, significant differences in DNA amounts were observed for TPAs and SPAs, suggesting a better performance of MSCs on TPAs after reseeding. Although the cell growth on BPXs also showed a tentative increase up to 14 days (796.5 ng), DNA quantification data did not reveal significant differences for the investigated time points. Similar amounts of DNA were observed on day 1 for TPAs, SPAs and BPXs suggesting that the initial adhesion is comparable.

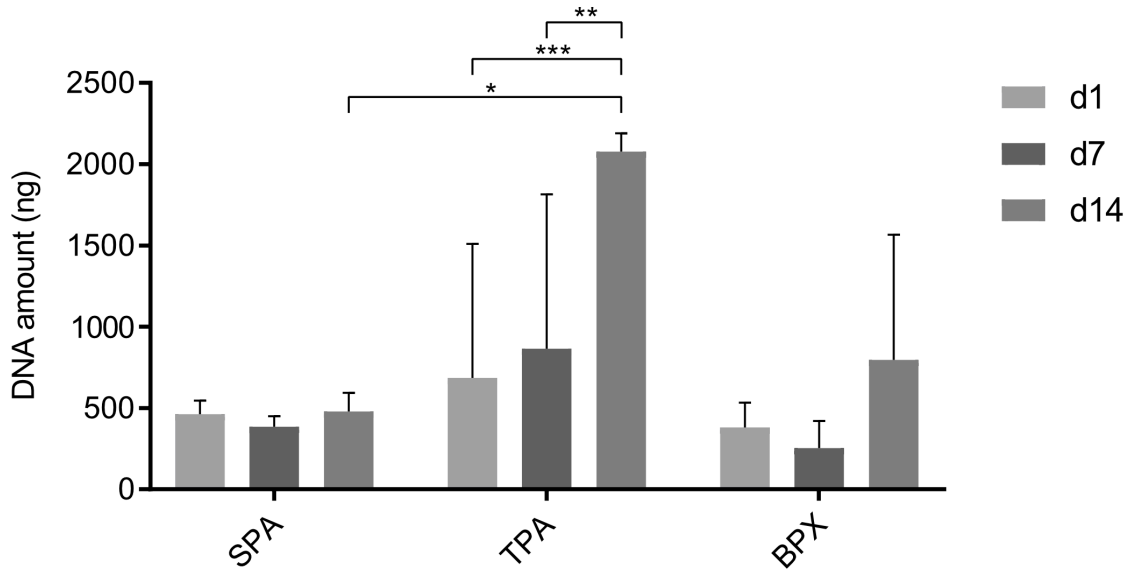

Figure 15. DNA quantification of mesenchymal stem cells 1, 7 and 14 days after seeding onto sonication-based processed allografts, Tutoplast processed allografts and Bio-Oss processed xenografts. Tutoplast processed allografts show a significant increase in DNA from day 1 and

day 7 to day 14, suggesting proliferation of mesenchymal stem cells. Furthermore, DNA levels differed significantly between sonication-based processed allografts and Tutoplast processed allografts on day 14 indicating better cell growth on Tutoplast processed allografts. DNA background values determined for empty grafts (compare Figure 5) were subtracted from values obtained after mesenchymal stem cell-seeding. Statistics are based on Tukey's multiple comparison in conjunction with ANOVA (n = 3 mesenchymal stem cell donors and 3 graft donors, two independent mesenchymal stem cell-seeded constructs were quantified per donor, * $p < 0.05$, ** $p < 0.01$, *** $p < 0.001$).

3.2.4 Osteogenic activity determined by ALP assay

Furthermore, ALP activity as an early marker for osteogenic differentiation was measured in order to assess MSC functionality on the grafts (Figure 16A). For this purpose, medium retrieved from MSC-seeded constructs was collected on day 1, 7 and day 14 and ALP levels were normalized to the corresponding DNA content (compare Figure 15) in order to cope with a potential impact of the cell numbers on the ALP activity. BPXs displayed a tentative, yet non-significant increase of normalized ALP activity from day 1 to day 7. ALP levels of SPAs showed no significant increase or decrease throughout the 14-day period while TPAs showed a significant decrease from day 1 to day 14 in the alkaline phosphatase activity as early osteogenic marker.

3.2.5 Quantification of mineralization of cell seeded constructs by Alizarin Red S

Mineralization of MSC-seeded grafts was assessed by Alizarin Red S (Figure 16B) and included the subtraction of background values derived from grafts before cell seeding (see Supplemental Figure 1). Additionally, Alizarin Red S levels were normalized to the corresponding DNA content (Figure 16B, upper graph) to cope with a potential impact of the cell numbers on the degree of mineralization (compare Fig 15). After normalization to the DNA content, BPXs displayed a tentative yet non-significant increase in mineralization from 26.6 mM/µg DNA on day 7 to 69.3 mM/µg DNA on day 14. However, increased mineralization levels for both BPXs and TPAs were documented when alizarin quantification was not normalized to DNA content (Figure 15B, lower graph).

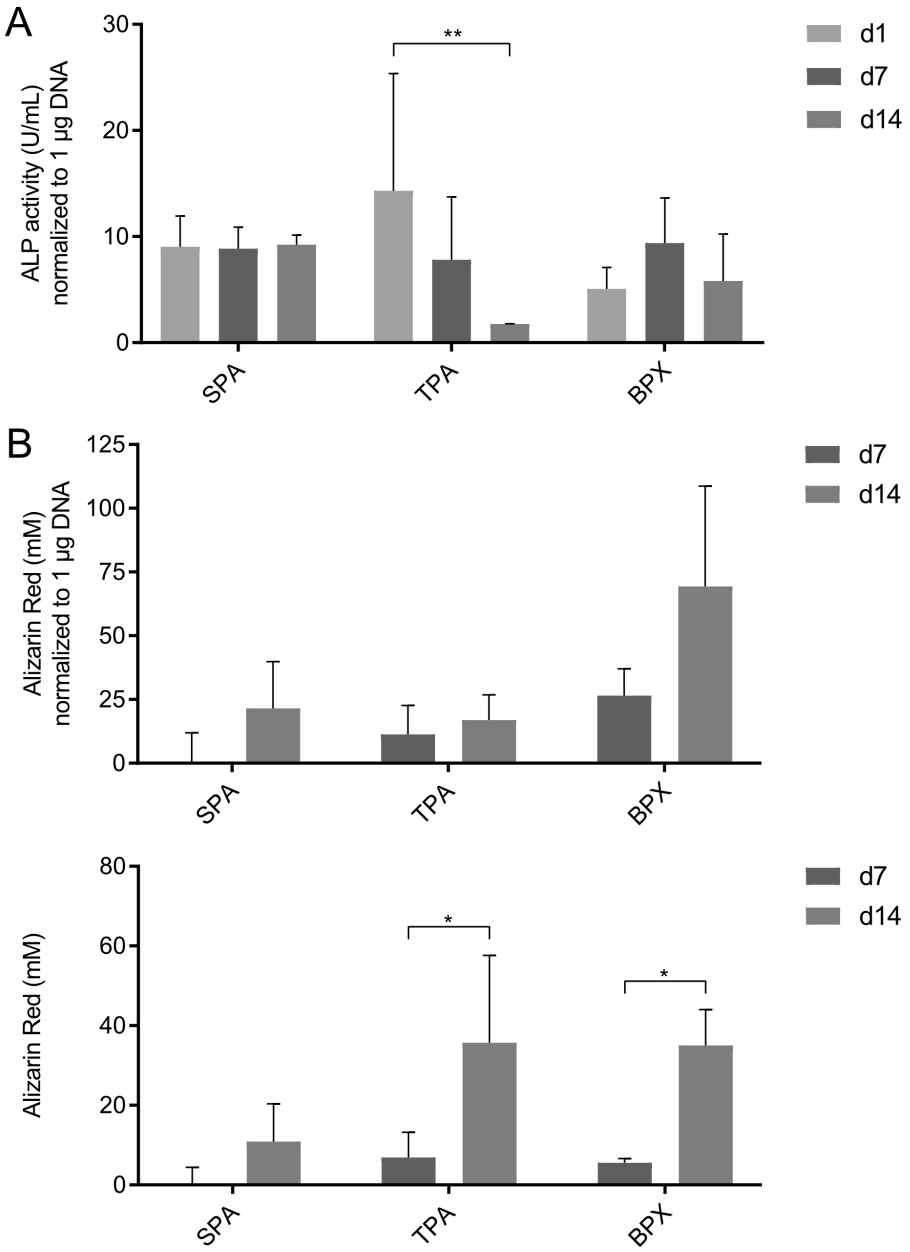

Figure 16. Alkaline phosphatase quantification (A) of cell-seeded constructs 1, 7 and 14 days and Alizarin Red S quantification (B) 7 and 14 days after seeding mesenchymal stem cells onto sonication-based processed allografts, Tutoplast processed allografts and Bio-Oss processed xenografts. (A) Alkaline phosphatase quantification was performed from supernatant retrieved from seeded grafts on day 1, 7 and 14. Alkaline phosphatase levels were normalized to DNA amount (compare Figure 14). Bio-Oss processed xenografts show the highest tentative, yet non-significant increase in Alkaline phosphatase levels from day 1 to day 7. Tutoplast processed allografts show a significant decrease from day 1 to day 14. (B) Alizarin Red S values were also normalized to corresponding DNA levels (Figure 15B, upper graph). Normalized data indicate the most prominent yet non-significant increase in calcification for Bio-Oss processed xenografts. Alizarin Red S data not normalized to DNA however (Figure 15B, lower graph) indicate a significant increase in calcification for both Bio-Oss processed xenografts and Tutoplast processed allografts. Statistics are based on Tukey's multiple comparison in conjunction with ANOVA (n = 3 mesenchymal stem cell donors and 3 graft donors, two independent mesenchymal stem cell-seeded constructs were quantified per donor, * $p < 0.05$, ** $p < 0.01$).

4. Discussion

4.1 Assessment of degree of decellularization

The increased incidence of bone defects, especially in cases of comminuted fractures or non-unions demand suitable bone grafts and therefore rising amounts of suitable allografts are required. Currently, several decellularization methods for allografts have been proposed but it still remains unclear which method results in favorable physiochemical properties or might be preferred in stem cell applications. Hence, the aim of this study was firstly to compare two decellularization methods concerning their decellularization capacity for bone grafts, and secondly, to investigate their impact on MSC functionality together with two commercially available grafts.

4.1.1 Comparing decellularization of chemically processed allografts to sonication-based processed allografts

Based on histological examination, SEM examination and DNA quantification, a higher efficacy in decellularization could be shown for SPAs in comparison to CPAs. This was documented by significantly higher amounts of DNA after decellularization in CPAs compared to SPAs, although CPAs were treated with DNase in an additional step. Similarly, SEM images revealed marrow cavities filled with tissue, underscoring incomplete decellularization in CPAs. SPAs, on the other hand, showed empty marrow cavities, revealing a rough surface structure and distinct trabecular structures. The increased clearance of marrow cavities in SPAs over CPAs might be due to the disrupting effect of sonication on cell membranes [116]. Additionally, mechanical energy exerted by sonication possibly helped to clear any residues [117]. In this study we treated SPAs, as mentioned above, by sonicating grafts at 20 kHz with an amplitude of 12 microns. This is in accordance to previous reports showing this frequency to have a cell membrane disrupting effect and a significant reduction in cell viability [116,118]. It is important to note that the efficacy of decellularization for SPAs in our experiments was comparable to TPAs and BPXs as commercial standardized products.

4.1.2 Decellularization of Tutoplast® processed allografts and Bio-Oss® processed xenografts

Commercially available TPAs are generated by a combination of chemical and physical treatment steps including sonication, acetone treatment, osmotic treatment, sterilization via hydrogen peroxide solutions, serial dehydration and gamma irradiation [109,119]. BPXs differ from all other grafts as they originate from a bovine source and are treated with heat (300°C), alkaline chemicals and sterilization using dry heart [119]. This process is supposed to remove any proteins or antigenic structures [120]. Nevertheless, assessment of protein content, or the presence of immune response mediating material was not in the scope of this present study.

4.2 Biocompatibility issues

Initial biocompatibility testing based on extraction medium from grafts showed unsatisfactory levels of cell viability at ~ 1% to ~ 16% in CPAs and SPAs (Figure 8). BPXs, as reference for a commercially available graft, showed levels at ~ 50% while untreated medium was used as negative control (100%). Though the decrease of cell viability might be due to a variety of different agents acting in a biological, chemical or physical manner, the proposal was made to centrifuge extracts at 12,000 x g for 5 min in an effort to increase cell viability. Differential centrifugation at ~ 10,000 x g is known to form a pellet with mitochondria and subcellular particles [121], as well as particles with a larger size, such as cells [122] or bone debris [123] which already separate at lower speeds. However, centrifuging the extracts before addition to MSCs did not show an increase in cell viability (compare Figure 9 and Figure 12). In an attempt to remove any cell viability reducing agent which could induce apoptosis, extracts were sterile filtered with a pore size of 0.2 μm. Seeing as how this approach did not increase cell viability either (see Figure 10), a change of protocol concerning the storage of the grafts after decellularization was performed. Initially, before CPAs and SPAs were used in experiments, they were stored at -80°C for practical reasons. It was proposed, that this re-freezing could have an effect on the integrity of the graft and lead to the liberation of harmful substances. Thus, in-between storage was kept to a minimum and performed at 4°C. This change in protocol significantly raised the cell viability of both CPAs and SPAs to ~ 50% to ~ 60% (see Figure 11 and Figure 12), being comparable to cell viability values of BPXs. Even though BPXs were never frozen, as they were

acquired commercially and stored at room temperature, extracts derived from BPXs did not show a significant increase in cell viability when extracts were treated as mentioned above.

The only graft showing no reduction in cell viability compared to controls were TPAs (Figure 11). Results for TPAs are congruent with other published data showing favorable cell viability properties for TPAs [107,124].

Even though changing the protocol from storage at -80°C to storage at 4°C significantly increased the cell viability in CPAs and SPAs to ~ 50% to ~ 60%, cell viability levels still differed significantly from controls. This reduction of cell viability in CPAs, SPAs and also BPXs might be due to a variety of different reasons and its underlying biological mechanisms.

4.2.1 Biocompatibility of chemically processed allografts and sonication-based processed allografts

The reduction in MSC viability for CPA extracts might be caused by chemical substances such as Triton X-100 and SDS, used in the decellularization process leaking out even after thorough washing. On the other hand many potential mediators such as TNF-α [125], cytochrome c [126] and miRNA released by cells during the decellularization method, or in not completely decellularized materials, might lead to reduced cell viability in MSCs treated with the extracts. Although the procedure includes intensive washing, an impact of such molecules cannot be excluded but might be determined in future studies.

4.2.2 Biocompatibility of Bio-Oss® processed xenografts

BPX extracts also induced a reduction in MSC cell viability. As BPXs have been shown to be void of any cellular material (Figure 4), and as a result, the above-mentioned explanations are not applicable to this graft. Though our findings are in line with other published data showing a reduction in cell viability [127,128], to our knowledge, no explanation has yet been given. Considering that BPXs mainly consist of hydroxyapatite and have a very porous consistency, a tentative explanation could constitute the induction of apoptosis by nanoparticles [129]. Even though our results regarding BPXs are consistent with *in vitro* data, it should be noted that a discrepancy between results from experiments *in vitro* and *in vivo* cannot be excluded. While *in*

vitro testing often offers the ability to study cellular and molecular processes more closely, a direct translation to an *in vivo* setting might often be limited. In fact, BPXs have repeatedly been shown to integrate well *in vivo* by demonstrating large quantities of osteoid matrix depositions and being enveloped well by adjacent tissue [130,131].

4.3 Mesenchymal stem cell functionality

The impact of graft processing on the graft's ability to host MSCs was assessed by examining cell morphology and cell density of seeded MSCs.

4.3.1 MSC morphology and proliferation rate on Tutoplast® processed allografts

CLSM revealed an elongated and spindle-like morphology of MSCs with a high cell density on SPAs and TPAs.

DNA quantification to monitor cell adhesion and proliferation on the different grafts in a quantitative manner indicated the best MSC growth and proliferation on TPAs. These data were further supported by the MTS data for the TPA extracts indicating a good biocompatibility and viability levels close to the controls, as well as by the morphological assessment as described above. Further DNA quantification demonstrated that the initial adhesion was similar for all tested constructs so that the good cell growth on TPAs might not be explained by differences in initial cell adhesion or technical issues associated with the seeding procedure.

4.3.2 Nitrogen levels as an indicator for organic material in Tutoplast® processed allografts and sonication-based processed allografts

In this context, EDX analysis of bone grafts indicated in TPAs the highest value for nitrogen and conversely the lowest Ca/N ratios, followed by SPAs. Human bone is composed of a mineral phase (hydroxyapatite), an organic phase (mainly collagen type I) and water [96]. A high At% of nitrogen, ubiquitous in organic compounds, might correlate with a high amount of collagen [132] in TPAs and SPAs. MSCs, at the same time, readily adhere to collagen type I [133]. This in turn could explain superior properties for MSC functionality in regard to TPAs but not for SPAs.

4.3.3 Mesenchymal stem cell functionality of Bio-Oss® processed xenografts

BPXs displayed the highest At% of calcium and phosphorous. Yet, Ca/P ratios were similar for all grafts and did not differ significantly. Shih et al. showed that calcium phosphate rich bone grafts can induce osteogenesis via a phosphate-adenosine signaling pathway [106]. It is interesting to note that while BPXs showed the highest At% of calcium and phosphorous, they also demonstrated the highest tentative, yet non-significant increase in ALP activity. Additionally, quantification of mineralization by Alizarin Red S showed tentative (DNA normalized) respectively significant (not normalized) increase potentially associated with osteoinductive properties of calcium rich BPXs. Accordingly, BPXs showed high background values in Alizarin Red S assays. While this further substantiates the results from EDX spectroscopy, depicting BPXs as the grafts with the highest amount of Ca (Figure 5A), it also limits to some extent the interpretability of results on mineralization due to these high background levels despite subtraction.

4.4 Osteogenic activity

Biomineralization and hydroxyapatite deposition is well known to depend on ALP activity as it provides phosphates during these processes [93,95]. Furthermore, ALP is amongst the early markers of osteoblast differentiation which is highly prominent in the starting phase of the mineralization process [134,135] but undergoes a downregulation when mineralization progresses. Accordingly, the significant decrease of ALP activity in TPAs, along with the increase in mineralization (non-normalized data), reflects such a typical marker profile widely described for osteogenic differentiation of MSCs and further underlines the impact of TPAs on MSC functionality.

5. Summary

The outcome of this study shows a higher efficacy in decellularization for sonication-based processed allografts (SPAs) over chemically processed allografts (CPAs) based on DNA quantification, histological and scanning electron microscopy (SEM) evaluation. Moreover, the decellularization efficacy of SPAs was comparable to two commercial grafts, Tutoplast® processed allografts (TPAs) and Bio-Oss® processed

xenografts (BPXs), used as additional reference, also in terms of commercially standardized products. Biocompatibility assessment based on extracts derived from decellularized grafts showed a decrease in mesenchymal stem cell (MSC) viability for SPAs and CPAs, as well as for the commercially available BPXs. In contrast, biocompatibility was not impaired for TPAs, which also showed a better performance after reseeding with MSCs as indicated by confocal laser scanning microscopy (CSLM) and DNA assessment in order to monitor cellular proliferation. Here, a significant increase in DNA throughout a two-week time frame could be shown. BPXs induced a tentative increase in alkaline phosphatase (ALP) activity and mineralization in MSCs potentially associated with the high calcium content. Even though SPAs extracts showed a noticeable reduction of *in vitro* biocompatibility, results after reseeding with MSCs were comparable to commercially available grafts used in this study. Nevertheless, in this present study, TPAs combined the best *in vitro* biocompatibility and performance in terms of proliferation and osteogenic differentiation after reseeding with MSCs.

6. Supplemental Material

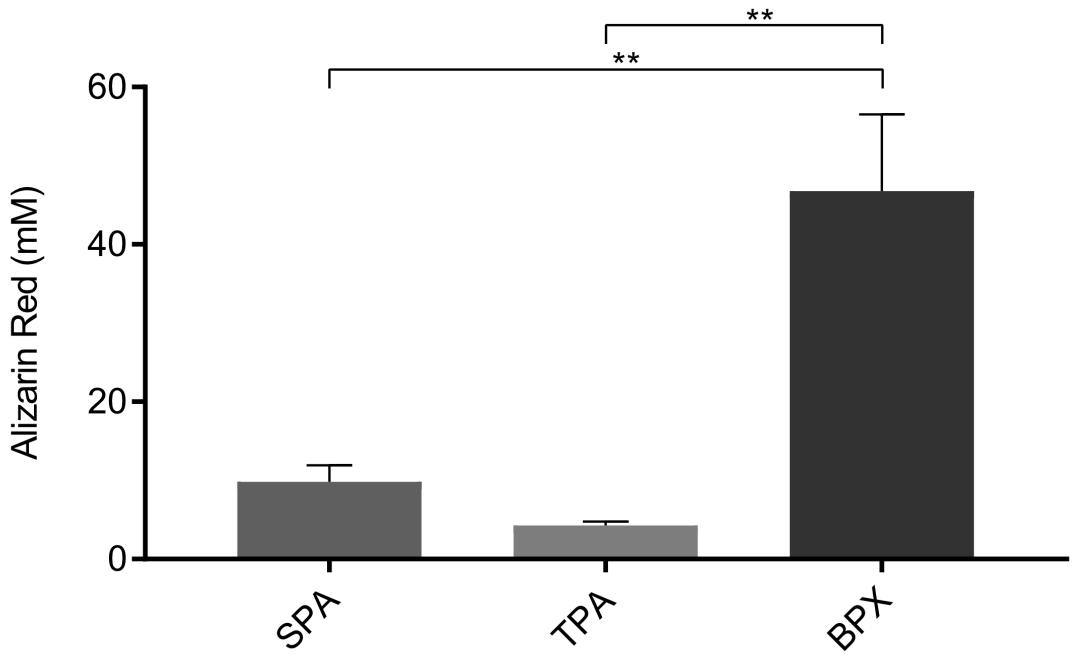

Supplemental figure 1. Alizarin Red S quantification of un-seeded sonication-based processed allografts, Tutoplast processed allografts and Bio-Oss processed xenografts as background. Background values of Alizarin Red S quantification were obtained by staining un-seeded grafts with Alizarin Red S solution and consecutively extracting and photocolorimetrically measuring the Alizarin Red S that attached to the un-seeded grafts. Bio-Oss processed xenografts show the highest values, differing significantly to all other grafts. Tutoplast processed allografts on the other hand, display the lowest values. Statistics are based on Tukey's multiple comparison in conjunction with ANOVA (n = 3, ** p < 0.01).

7. References

1. United States Bone and Joint Initiative. The Burden of Musculoskeletal Diseases in the United States (BMUS), (Third Edition) [Internet]. Rosemont, IL ; [cited 15 February 2019],
   Available from: https://www.boneandjointburden.org/resources/archives
2. Curtis EM, van der Velde R, Moon RJ, van den Bergh JP, Geusens P, de Vries F, et al. Epidemiology of fractures in the United Kingdom 1988-2012: Variation with age, sex, geography, ethnicity and socioeconomic status. Bone. 2016/03/13. 2016;87:19–26.
3. Marsell R, Einhorn TA. The biology of fracture healing. Injury. 2011/04/15. 2011;42(6):551–5.
4. Einhorn TA, Gerstenfeld LC. Fracture healing: mechanisms and interventions. Nat Rev Rheumatol. 2014/10/01. 2015;11(1):45–54.
5. Wiese A, Pape HC. Bone defects caused by high-energy injuries, bone loss, infected nonunions, and nonunions. Orthop Clin North Am. 2009/11/26. 2010;41(1):1–4, table of contents.
6. Bauer TW, Muschler GF. Bone graft materials. An overview of the basic science. Clin Orthop Relat Res. 2000/02/29. 2000;(371):10–27.
7. Cypher TJ, Grossman JP. Biological principles of bone graft healing. J Foot Ankle Surg. 1996/09/01. 1996;35(5):413–7.
8. Homma Y, Zimmermann G, Hernigou P. Cellular therapies for the treatment of non-union: the past, present and future. Injury. 2013/02/13. 2013;44 Suppl 1:S46-9.
9. Delloye C, Cornu O, Druez V, Barbier O. Bone allografts: What they can offer and what they cannot. J Bone Jt Surg (British Vol. 2007/06/02. 2007;89(5):574–9.
10. Campana V, Milano G, Pagano E, Barba M, Cicione C, Salonna G, et al. Bone substitutes in orthopaedic surgery: from basic science to clinical practice. J Mater Sci Mater Med. 2014/05/29. 2014;25(10):2445–61.
11. Deijkers RL, Bouma GJ, van der Meer-Prins EM, Huysmans PE, Taminiau AH, Claas FH. Human bone allografts can induce T cells with high affinity for donor antigens. J Bone Jt Surg (British Vol. 2000/06/29. 1999;81(3):538–44.
12. Griesemer A, Yamada K, Sykes M. Xenotransplantation: immunological hurdles and progress toward tolerance. Immunol Rev. 2014/02/13. 2014;258(1):241–58.
13. Smith CA, Board TN, Rooney P, Eagle MJ, Richardson SM, Hoyland JA. Human decellularized bone scaffolds from aged donors show improved osteoinductive capacity compared to young donor bone. PLoS One. 2017/05/16. 2017;12(5):e0177416.
14. Saulacic N, Bosshardt DD, Jensen SS, Miron RJ, Gruber R, Buser D. Impact of bone graft harvesting techniques on bone formation and graft resorption: a histomorphometric study in the mandibles of minipigs. Clin Oral Implants Res.

2014/02/20. 2015;26(4):383–91.
15. do Desterro Fde P, Sader MS, Soares GD, Vidigal Jr. GM. Can inorganic bovine bone grafts present distinct properties? Braz Dent J. 2014/09/25. 2014;25(4):282–8.
16. Boyce T, Edwards J, Scarborough N. Allograft bone. The influence of processing on safety and performance. Orthop Clin North Am. 1999/09/03. 1999;30(4):571–81.
17. Worth A, Mucalo M, Horne G, Bruce W, Burbidge H. The evaluation of processed cancellous bovine bone as a bone graft substitute. Clin Oral Implants Res. 2005/05/10. 2005;16(3):379–86.
18. Ullah I, Subbarao RB, Rho GJ. Human mesenchymal stem cells - current trends and future prospective. Biosci Rep. 2015/03/24. 2015;35(2).
19. Friedenstein AJ, Chailakhjan RK, Lalykina KS. The development of fibroblast colonies in monolayer cultures of guinea-pig bone marrow and spleen cells. Cell Tissue Kinet. 1970/10/01. 1970;3(4):393–403.
20. Friedenstein AJ, Piatetzky II S, Petrakova K V. Osteogenesis in transplants of bone marrow cells. J Embryol Exp Morphol. 1966/12/01. 1966;16(3):381–90.
21. McDaniel JS, Antebi B, Pilia M, Hurtgen BJ, Belenkiy S, Necsoiu C, et al. Quantitative Assessment of Optimal Bone Marrow Site for the Isolation of Porcine Mesenchymal Stem Cells. Stem Cells Int. 2017/05/26. 2017;2017:1836960.
22. Wagner W, Wein F, Seckinger A, Frankhauser M, Wirkner U, Krause U, et al. Comparative characteristics of mesenchymal stem cells from human bone marrow, adipose tissue, and umbilical cord blood. Exp Hematol. 2005/11/03. 2005;33(11):1402–16.
23. Zhang X, Yang M, Lin L, Chen P, Ma KT, Zhou CY, et al. Runx2 overexpression enhances osteoblastic differentiation and mineralization in adipose--derived stem cells in vitro and in vivo. Calcif Tissue Int. 2006/09/14. 2006;79(3):169–78.
24. Ab Kadir R, Zainal Ariffin SH, Megat Abdul Wahab R, Kermani S, Senafi S. Characterization of mononucleated human peripheral blood cells. ScientificWorldJournal. 2012/06/06. 2012;2012:843843.
25. Huang GT, Gronthos S, Shi S. Mesenchymal stem cells derived from dental tissues vs. those from other sources: their biology and role in regenerative medicine. J Dent Res. 2009/09/22. 2009;88(9):792–806.
26. Morito T, Muneta T, Hara K, Ju YJ, Mochizuki T, Makino H, et al. Synovial fluid-derived mesenchymal stem cells increase after intra-articular ligament injury in humans. Rheumatol. 2008/04/09. 2008;47(8):1137–43.
27. In 't Anker PS, Scherjon SA, Kleijburg-van der Keur C, Noort WA, Claas FH, Willemze R, et al. Amniotic fluid as a novel source of mesenchymal stem cells for therapeutic transplantation. Blood. 2003/08/06. 2003;102(4):1548–9.
28. Wang HS, Hung SC, Peng ST, Huang CC, Wei HM, Guo YJ, et al. Mesenchymal stem cells in the Wharton's jelly of the human umbilical cord. Stem Cells. 2004/12/08. 2004;22(7):1330–7.

29. Raynaud CM, Maleki M, Lis R, Ahmed B, Al-Azwani I, Malek J, et al. Comprehensive characterization of mesenchymal stem cells from human placenta and fetal membrane and their response to osteoactivin stimulation. Stem Cells Int. 2012/06/16. 2012;2012:658356.
30. da Silva Meirelles L, Chagastelles PC, Nardi NB. Mesenchymal stem cells reside in virtually all post-natal organs and tissues. J Cell Sci. 2006/05/11. 2006;119(Pt 11):2204–13.
31. Yin Z, Guo J, Wu TY, Chen X, Xu LL, Lin SE, et al. Stepwise Differentiation of Mesenchymal Stem Cells Augments Tendon-Like Tissue Formation and Defect Repair In Vivo. Stem Cells Transl Med. 2016/06/10. 2016;5(8):1106–16.
32. Hodgson B, Mafi R, Mafi P, Khan. The Regulation of Differentiation of Mesenchymal Stem-cells into Skeletal Muscle: A Look at Signalling Molecules Involved in Myogenesis. Curr Stem Cell Res Ther. 2017/09/12. 2018;13(5):384–407.
33. Mafi R, Hindocha S, Mafi P, Griffin M, Khan WS. Sources of adult mesenchymal stem cells applicable for musculoskeletal applications - a systematic review of the literature. Open Orthop J. 2011/09/03. 2011;5 Suppl 2:242–8.
34. Shi C. Recent progress toward understanding the physiological function of bone marrow mesenchymal stem cells. Immunology. 2012/02/11. 2012;136(2):133–8.
35. Dominici M, Le Blanc K, Mueller I, Slaper-Cortenbach I, Marini F, Krause D, et al. Minimal criteria for defining multipotent mesenchymal stromal cells. The International Society for Cellular Therapy position statement. Cytotherapy. 2006/08/23. 2006;8(4):315–7.
36. Hare JM, Traverse JH, Henry TD, Dib N, Strumpf RK, Schulman SP, et al. A randomized, double-blind, placebo-controlled, dose-escalation study of intravenous adult human mesenchymal stem cells (prochymal) after acute myocardial infarction. J Am Coll Cardiol. 2009/12/05. 2009;54(24):2277–86.
37. White IA, Sanina C, Balkan W, Hare JM. Mesenchymal Stem Cells in Cardiology. Methods Mol Biol. 2016/05/30. 2016;1416:55–87.
38. Morigi M, Benigni A, Remuzzi G, Imberti B. The regenerative potential of stem cells in acute renal failure. Cell Transpl. 2006/07/11. 2006;15 Suppl 1:S111-7.
39. Morigi M, Rota C, Remuzzi G. Mesenchymal Stem Cells in Kidney Repair. Methods Mol Biol. 2016/05/30. 2016;1416:89–107.
40. Xu P, Yang X. The Efficacy and Safety of Mesenchymal Stem Cell Transplantation for Spinal Cord Injury Patients: A Meta-Analysis and Systematic Review. Cell Transpl. 2018/10/27. 2019;28(1):36–46.
41. Karnieli O, Izhar-Prato Y, Bulvik S, Efrat S. Generation of insulin-producing cells from human bone marrow mesenchymal stem cells by genetic manipulation. Stem Cells. 2007/07/07. 2007;25(11):2837–44.
42. Si Y, Zhao Y, Hao H, Liu J, Guo Y, Mu Y, et al. Infusion of mesenchymal stem cells ameliorates hyperglycemia in type 2 diabetic rats: identification of a novel role in improving insulin sensitivity. Diabetes. 2012/05/24. 2012;61(6):1616–25.
43. Chahal J, Gomez-Aristizabal A, Shestopaloff K, Bhatt S, Chaboureau A, Fazio

A, et al. Bone Marrow Mesenchymal Stromal Cell Treatment in Patients with Osteoarthritis Results in Overall Improvement in Pain and Symptoms and Reduces Synovial Inflammation. Stem Cells Transl Med. 2019/04/10. 2019;8(8):746–57.
44. Iijima H, Isho T, Kuroki H, Takahashi M, Aoyama T. Effectiveness of mesenchymal stem cells for treating patients with knee osteoarthritis: a meta-analysis toward the establishment of effective regenerative rehabilitation. NPJ Regen Med. 2018/09/25. 2018;3:15.
45. Bhumiratana S, Eton RE, Oungoulian SR, Wan LQ, Ateshian GA, Vunjak-Novakovic G. Large, stratified, and mechanically functional human cartilage grown in vitro by mesenchymal condensation. Proc Natl Acad Sci U S A. 2014/04/30. 2014;111(19):6940–5.
46. Horwitz EM, Prockop DJ, Fitzpatrick LA, Koo WW, Gordon PL, Neel M, et al. Transplantability and therapeutic effects of bone marrow-derived mesenchymal cells in children with osteogenesis imperfecta. Nat Med. 1999/03/23. 1999;5(3):309–13.
47. Zhao D, Cui D, Wang B, Tian F, Guo L, Yang L, et al. Treatment of early stage osteonecrosis of the femoral head with autologous implantation of bone marrow-derived and cultured mesenchymal stem cells. Bone. 2011/11/19. 2012;50(1):325–30.
48. Rackwitz L, Eden L, Reppenhagen S, Reichert JC, Jakob F, Walles H, et al. Stem cell- and growth factor-based regenerative therapies for avascular necrosis of the femoral head. Stem Cell Res Ther. 2012/02/24. 2012;3(1):7.
49. Ismail HD, Phedy P, Kholinne E, Djaja YP, Kusnadi Y, Merlina M, et al. Mesenchymal stem cell implantation in atrophic nonunion of the long bones: A translational study. Bone Jt Res. 2016/07/15. 2016;5(7):287–93.
50. Jin YZ, Lee JH. Mesenchymal Stem Cell Therapy for Bone Regeneration. Clin Orthop Surg. 2018/09/04. 2018;10(3):271–8.
51. Kon E, Muraglia A, Corsi A, Bianco P, Marcacci M, Martin I, et al. Autologous bone marrow stromal cells loaded onto porous hydroxyapatite ceramic accelerate bone repair in critical-size defects of sheep long bones. J Biomed Mater Res. 1999/12/22. 2000;49(3):328–37.
52. Quarto R, Giannoni P. Bone Tissue Engineering: Past-Present-Future. Methods Mol Biol. 2016/05/30. 2016;1416:21–33.
53. Gjerde C, Mustafa K, Hellem S, Rojewski M, Gjengedal H, Yassin MA, et al. Cell therapy induced regeneration of severely atrophied mandibular bone in a clinical trial. Stem Cell Res Ther. 2018/08/11. 2018;9(1):213.
54. Mangano FG, Colombo M, Veronesi G, Caprioglio A, Mangano C. Mesenchymal stem cells in maxillary sinus augmentation: A systematic review with meta-analysis. World J Stem Cells. 2015/08/05. 2015;7(6):976–91.
55. Ren G, Zhang L, Zhao X, Xu G, Zhang Y, Roberts AI, et al. Mesenchymal stem cell-mediated immunosuppression occurs via concerted action of chemokines and nitric oxide. Cell Stem Cell. 2008/03/29. 2008;2(2):141–50.

56. Jacobs SA, Roobrouck VD, Verfaillie CM, Van Gool SW. Immunological characteristics of human mesenchymal stem cells and multipotent adult progenitor cells. Immunol Cell Biol. 2013/01/09. 2013;91(1):32–9.
57. Campeau PM, Rafei M, Francois M, Birman E, Forner KA, Galipeau J. Mesenchymal stromal cells engineered to express erythropoietin induce anti-erythropoietin antibodies and anemia in allorecipients. Mol Ther. 2008/12/18. 2009;17(2):369–72.
58. Zangi L, Margalit R, Reich-Zeliger S, Bachar-Lustig E, Beilhack A, Negrin R, et al. Direct imaging of immune rejection and memory induction by allogeneic mesenchymal stromal cells. Stem Cells. 2009/09/15. 2009;27(11):2865–74.
59. Ankrum JA, Ong JF, Karp JM. Mesenchymal stem cells: immune evasive, not immune privileged. Nat Biotechnol. 2014/02/25. 2014;32(3):252–60.
60. Garcia-Olmo D, Garcia-Arranz M, Herreros D, Pascual I, Peiro C, Rodriguez-Montes JA. A phase I clinical trial of the treatment of Crohn's fistula by adipose mesenchymal stem cell transplantation. Dis Colon Rectum. 2005/06/04. 2005;48(7):1416–23.
61. Mohyeddin Bonab M, Yazdanbakhsh S, Lotfi J, Alimoghaddom K, Talebian F, Hooshmand F, et al. Does mesenchymal stem cell therapy help multiple sclerosis patients? Report of a pilot study. Iran J Immunol. 2007/07/27. 2007;4(1):50–7.
62. Karussis D, Karageorgiou C, Vaknin-Dembinsky A, Gowda-Kurkalli B, Gomori JM, Kassis I, et al. Safety and immunological effects of mesenchymal stem cell transplantation in patients with multiple sclerosis and amyotrophic lateral sclerosis. Arch Neurol. 2010/10/13. 2010;67(10):1187–94.
63. Ringden O, Uzunel M, Rasmusson I, Remberger M, Sundberg B, Lonnies H, et al. Mesenchymal stem cells for treatment of therapy-resistant graft-versus-host disease. Transplantation. 2006/05/30. 2006;81(10):1390–7.
64. Schell H, Duda GN, Peters A, Tsitsilonis S, Johnson KA, Schmidt-Bleek K. The haematoma and its role in bone healing. J Exp Orthop. 2017/02/09. 2017;4(1):5.
65. Kolar P, Gaber T, Perka C, Duda GN, Buttgereit F. Human early fracture hematoma is characterized by inflammation and hypoxia. Clin Orthop Relat Res. 2011/03/17. 2011;469(11):3118–26.
66. Dimitriou R, Tsiridis E, Giannoudis P V. Current concepts of molecular aspects of bone healing. Injury. 2005/08/17. 2005;36(12):1392–404.
67. Su P, Tian Y, Yang C, Ma X, Wang X, Pei J, et al. Mesenchymal Stem Cell Migration during Bone Formation and Bone Diseases Therapy. Int J Mol Sci. 2018/08/12. 2018;19(8).
68. Wynn RF, Hart CA, Corradi-Perini C, O'Neill L, Evans CA, Wraith JE, et al. A small proportion of mesenchymal stem cells strongly expresses functionally active CXCR4 receptor capable of promoting migration to bone marrow. Blood. 2004/07/15. 2004;104(9):2643–5.
69. Kitaori T, Ito H, Schwarz EM, Tsutsumi R, Yoshitomi H, Oishi S, et al. Stromal cell-derived factor 1/CXCR4 signaling is critical for the recruitment of

mesenchymal stem cells to the fracture site during skeletal repair in a mouse model. Arthritis Rheum. 2009/02/28. 2009;60(3):813–23.
70. Toupadakis CA, Wong A, Genetos DC, Chung DJ, Murugesh D, Anderson MJ, et al. Long-term administration of AMD3100, an antagonist of SDF-1/CXCR4 signaling, alters fracture repair. J Orthop Res. 2012/05/18. 2012;30(11):1853–9.
71. Knight MN, Hankenson KD. Mesenchymal Stem Cells in Bone Regeneration. Adv Wound Care (New Rochelle). 2014/02/15. 2013;2(6):306–16.
72. Oh M, Nor JE. The Perivascular Niche and Self-Renewal of Stem Cells. Front Physiol. 2015/12/24. 2015;6:367.
73. Crisan M, Yap S, Casteilla L, Chen CW, Corselli M, Park TS, et al. A perivascular origin for mesenchymal stem cells in multiple human organs. Cell Stem Cell. 2008/09/13. 2008;3(3):301–13.
74. Sabatini F, Petecchia L, Tavian M, Jodon de Villeroche V, Rossi GA, Brouty-Boye D. Human bronchial fibroblasts exhibit a mesenchymal stem cell phenotype and multilineage differentiating potentialities. Lab Invest. 2005/06/01. 2005;85(8):962–71.
75. Otsuru S, Tamai K, Yamazaki T, Yoshikawa H, Kaneda Y. Bone marrow-derived osteoblast progenitor cells in circulating blood contribute to ectopic bone formation in mice. Biochem Biophys Res Commun. 2007/01/24. 2007;354(2):453–8.
76. Wan C, He Q, Li G. Allogenic peripheral blood derived mesenchymal stem cells (MSCs) enhance bone regeneration in rabbit ulna critical-sized bone defect model. J Orthop Res. 2006/03/04. 2006;24(4):610–8.
77. Edderkaoui B. Potential Role of Chemokines in Fracture Repair. Front Endocrinol. 2017/03/18. 2017;8:39.
78. Ceradini DJ, Kulkarni AR, Callaghan MJ, Tepper OM, Bastidas N, Kleinman ME, et al. Progenitor cell trafficking is regulated by hypoxic gradients through HIF-1 induction of SDF-1. Nat Med. 2004/07/06. 2004;10(8):858–64.
79. Wan C, Gilbert SR, Wang Y, Cao X, Shen X, Ramaswamy G, et al. Activation of the hypoxia-inducible factor-1alpha pathway accelerates bone regeneration. Proc Natl Acad Sci U S A. 2008/01/11. 2008;105(2):686–91.
80. Filipowska J, Tomaszewski KA, Niedzwiedzki L, Walocha JA, Niedzwiedzki T. The role of vasculature in bone development, regeneration and proper systemic functioning. Angiogenesis. 2017/02/15. 2017;20(3):291–302.
81. Ge Q, Zhang H, Hou J, Wan L, Cheng W, Wang X, et al. VEGF secreted by mesenchymal stem cells mediates the differentiation of endothelial progenitor cells into endothelial cells via paracrine mechanisms. Mol Med Rep. 2017/11/16. 2018;17(1):1667–75.
82. Bruder SP, Fink DJ, Caplan AI. Mesenchymal stem cells in bone development, bone repair, and skeletal regeneration therapy. J Cell Biochem. 1994/11/01. 1994;56(3):283–94.
83. Chen Q, Shou P, Zheng C, Jiang M, Cao G, Yang Q, et al. Fate decision of mesenchymal stem cells: adipocytes or osteoblasts? Cell Death Differ.

2016/02/13. 2016;23(7):1128–39.
84. Coelho MJ, Fernandes MH. Human bone cell cultures in biocompatibility testing. Part II: effect of ascorbic acid, beta-glycerophosphate and dexamethasone on osteoblastic differentiation. Biomaterials. 2000/05/19. 2000;21(11):1095–102.
85. Kim CH, Cheng SL, Kim GS. Effects of dexamethasone on proliferation, activity, and cytokine secretion of normal human bone marrow stromal cells: possible mechanisms of glucocorticoid-induced bone loss. J Endocrinol. 1999/09/01. 1999;162(3):371–9.
86. Bai Y, Li P, Yin G, Huang Z, Liao X, Chen X, et al. BMP-2, VEGF and bFGF synergistically promote the osteogenic differentiation of rat bone marrow-derived mesenchymal stem cells. Biotechnol Lett. 2012/11/13. 2013;35(3):301–8.
87. Li R, Liang L, Dou Y, Huang Z, Mo H, Wang Y, et al. Mechanical strain regulates osteogenic and adipogenic differentiation of bone marrow mesenchymal stem cells. Biomed Res Int. 2015/04/30. 2015;2015:873251.
88. Xu N, Liu H, Qu F, Fan J, Mao K, Yin Y, et al. Hypoxia inhibits the differentiation of mesenchymal stem cells into osteoblasts by activation of Notch signaling. Exp Mol Pathol. 2012/09/12. 2013;94(1):33–9.
89. Lee HH, Chang CC, Shieh MJ, Wang JP, Chen YT, Young TH, et al. Hypoxia enhances chondrogenesis and prevents terminal differentiation through PI3K/Akt/FoxO dependent anti-apoptotic effect. Sci Rep. 2013/09/18. 2013;3:2683.
90. Frank O, Heim M, Jakob M, Barbero A, Schafer D, Bendik I, et al. Real-time quantitative RT-PCR analysis of human bone marrow stromal cells during osteogenic differentiation in vitro. J Cell Biochem. 2002/04/23. 2002;85(4):737–46.
91. Vicari L, Calabrese G, Forte S, Giuffrida R, Colarossi C, Parrinello NL, et al. Potential Role of Activating Transcription Factor 5 during Osteogenesis. Stem Cells Int. 2016/01/16. 2016;2016:5282185.
92. Hanna H, Mir LM, Andre FM. In vitro osteoblastic differentiation of mesenchymal stem cells generates cell layers with distinct properties. Stem Cell Res Ther. 2018/07/29. 2018;9(1):203.
93. Sharma U, Pal D, Prasad R. Alkaline phosphatase: an overview. Indian J Clin Biochem. 2014/06/27. 2014;29(3):269–78.
94. Mornet E. Hypophosphatasia: the mutations in the tissue-nonspecific alkaline phosphatase gene. Hum Mutat. 2000/03/29. 2000;15(4):309–15.
95. E Golub E, Boesze-Battaglia K. The role of alkaline phosphatase in mineralization. Vol. 18. 2007. 444–448 p.
96. Boskey AL. Bone composition: relationship to bone fragility and antiosteoporotic drug effects. Bonekey Rep. 2014/02/07. 2013;2:447.
97. Polo-Corrales L, Latorre-Esteves M, Ramirez-Vick JE. Scaffold design for bone regeneration. J Nanosci Nanotechnol. 2014/04/16. 2014;14(1):15–56.
98. Zou L, Luo Y, Chen M, Wang G, Ding M, Petersen CC, et al. A simple method for deriving functional MSCs and applied for osteogenesis in 3D scaffolds. Sci

Rep. 2013/07/23. 2013;3:2243.
99. Oryan A, Baghaban Eslaminejad M, Kamali A, Hosseini S, Moshiri A, Baharvand H. Mesenchymal stem cells seeded onto tissue-engineered osteoinductive scaffolds enhance the healing process of critical-sized radial bone defects in rat. Cell Tissue Res. 2018/05/03. 2018;374(1):63–81.
100. Gao C, Harvey EJ, Chua M, Chen BP, Jiang F, Liu Y, et al. MSC-seeded dense collagen scaffolds with a bolus dose of VEGF promote healing of large bone defects. Eur Cell Mater. 2013/10/15. 2013;26:195–207; discussion 207.
101. Marcacci M, Kon E, Moukhachev V, Lavroukov A, Kutepov S, Quarto R, et al. Stem cells associated with macroporous bioceramics for long bone repair: 6- To 7-year outcome of a pilot clinical study. Tissue Eng. 2007;13(5):947–55.
102. Giannotti S, Trombi L, Bottai V, Ghilardi M, D'Alessandro D, Danti S, et al. Use of Autologous Human mesenchymal Stromal Cell/Fibrin Clot Constructs in Upper Limb Non-Unions: Long-Term Assessment. PLoS One. 2013 Aug 30;8(8).
103. Jones EA, Giannoudis P V., Kouroupis D. Bone repair with skeletal stem cells: rationale, progress to date and clinical application. Therapeutic Advances in Musculoskeletal Disease. 2016.
104. Murphy MB, Moncivais K, Caplan AI. Mesenchymal stem cells: environmentally responsive therapeutics for regenerative medicine. Exp Mol Med. 2013/11/16. 2013;45:e54.
105. Linero I, Chaparro O. Paracrine effect of mesenchymal stem cells derived from human adipose tissue in bone regeneration. PLoS One. 2014/09/10. 2014;9(9):e107001.
106. Shih YR, Hwang Y, Phadke A, Kang H, Hwang NS, Caro EJ, et al. Calcium phosphate-bearing matrices induce osteogenic differentiation of stem cells through adenosine signaling. Proc Natl Acad Sci U S A. 2014/01/08. 2014;111(3):990–5.
107. Seebach C, Schultheiss J, Wilhelm K, Frank J, Henrich D. Comparison of six bone-graft substitutes regarding to cell seeding efficiency, metabolism and growth behaviour of human mesenchymal stem cells (MSC) in vitro. Injury. 2010/03/18. 2010;41(7):731–8.
108. Harris CT, Cooper LF. Comparison of bone graft matrices for human mesenchymal stem cell-directed osteogenesis. J Biomed Mater Res Part A. 2004/02/27. 2004;68(4):747–55.
109. Mylonas D, Vidal MD, De Kok IJ, Moriarity JD, Cooper LF. Investigation of a thermoplastic polymeric carrier for bone tissue engineering using allogeneic mesenchymal stem cells in granular scaffolds. J Prosthodont. 2007/08/09. 2007;16(6):421–30.
110. Williams DF. On the mechanisms of biocompatibility. Biomaterials. 2008/04/29. 2008;29(20):2941–53.
111. Lin X, Chen J, Qiu P, Zhang Q, Wang S, Su M, et al. Biphasic hierarchical extracellular matrix scaffold for osteochondral defect regeneration. Osteoarthr Cartil. 2017/12/14. 2018;26(3):433–44.

112. Smith CA, Richardson SM, Eagle MJ, Rooney P, Board T, Hoyland JA. The use of a novel bone allograft wash process to generate a biocompatible, mechanically stable and osteoinductive biological scaffold for use in bone tissue engineering. J Tissue Eng Regen Med. 2014/06/20. 2015;9(5):595–604.
113. Vastel L, Meunier A, Siney H, Sedel L, Courpied JP. Effect of different sterilization processing methods on the mechanical properties of human cancellous bone allografts. Biomaterials. 2004/01/27. 2004;25(11):2105–10.
114. Wang F, Schmidt H, Pavleska D, Wermann T, Seekamp A, Fuchs S. Crude Fucoidan Extracts Impair Angiogenesis in Models Relevant for Bone Regeneration and Osteosarcoma via Reduction of VEGF and SDF-1. Mar Drugs. 2017/06/21. 2017;15(6).
115. Kolbe M, Xiang Z, Dohle E, Tonak M, Kirkpatrick CJ, Fuchs S. Paracrine effects influenced by cell culture medium and consequences on microvessel-like structures in cocultures of mesenchymal stem cells and outgrowth endothelial cells. Tissue Eng Part A. 2011/05/03. 2011;17(17–18):2199–212.
116. Sundaram J, Mellein BR, Mitragotri S. An experimental and theoretical analysis of ultrasound-induced permeabilization of cell membranes. Biophys J. 2003/04/30. 2003;84(5):3087–101.
117. Li D, Jiang S, Yin X, Chang JW, Ke J, Zhang C. Efficacy of Needle, Ultrasonic, and Endoactivator Irrigation and Photon-Induced Photoacoustic Streaming in Removing Calcium Hydroxide from the Main Canal and Isthmus: An In Vitro Micro-Computed Tomography and Scanning Electron Microscopy Study. Photomed Laser Surg. 2015/06/13. 2015;33(6):330–7.
118. Pong M, Umchid S, Guarino AJ, Lewin PA, Litniewski J, Nowicki A, et al. In vitro ultrasound-mediated leakage from phospholipid vesicles. Ultrasonics. 2006/09/19. 2006;45(1–4):133–45.
119. Moon KN, Kim SG, Oh JS, Kim CS, Lim SC, Jeong MA. Evaluation of bone formation after grafting with deproteinized bovine bone and mineralized allogenic bone. Implant Dent. 2015/01/27. 2015;24(1):101–5.
120. Benke D, Olah A, Mohler H. Protein-chemical analysis of Bio-Oss bone substitute and evidence on its carbonate content. Biomaterials. 2001/04/20. 2001;22(9):1005–12.
121. Lampl T, Crum JA, Davis TA, Milligan C, Del Gaizo Moore V. Isolation and functional analysis of mitochondria from cultured cells and mouse tissue. J Vis Exp. 2015/04/14. 2015;(97).
122. Lodish H Zipursky SL, et al. BA. Molecular Cell Biology. 4th edition. In New York: W. H. Freeman; 2000.
123. Helmers S, Sharkey PF, McGuigan FX. Efficacy of irrigation for removal of particulate debris after cemented total knee arthroplasty. J Arthroplast. 1999/09/04. 1999;14(5):549–52.
124. Mebarki M, Coquelin L, Layrolle P, Battaglia S, Tossou M, Hernigou P, et al. Enhanced human bone marrow mesenchymal stromal cell adhesion on scaffolds promotes cell survival and bone formation. Acta Biomater. 2017/06/22.

2017;59:94–107.
125. Rath PC, Aggarwal BB. TNF-induced signaling in apoptosis. J Clin Immunol. 2000/01/14. 1999;19(6):350–64.
126. Cai J, Yang J, Jones DP. Mitochondrial control of apoptosis: the role of cytochrome c. Biochim Biophys Acta. 1998/08/26. 1998;1366(1–2):139–49.
127. Bernhardt A, Lode A, Peters F, Gelinsky M. Novel ceramic bone replacement material Osbone(R) in a comparative in vitro study with osteoblasts. Clin Oral Implants Res. 2010/11/04. 2011;22(6):651–7.
128. Liu Q, Douglas T, Zamponi C, Becker ST, Sherry E, Sivananthan S, et al. Comparison of in vitro biocompatibility of NanoBone((R)) and BioOss((R)) for human osteoblasts. Clin Oral Implants Res. 2011/10/12. 2011;22(11):1259–64.
129. Jin Y, Liu X, Liu H, Chen S, Gao C, Ge K, et al. Oxidative stress-induced apoptosis of osteoblastic MC3T3-E1 cells by hydroxyapatite nanoparticles through lysosomal and mitochondrial pathways. RSC Adv. 2017;7(21):13010–8.
130. Wiltfang J, Rohnen M, Egberts JH, Lutzen U, Wieker H, Acil Y, et al. Man as a Living Bioreactor: Prefabrication of a Custom Vascularized Bone Graft in the Gastrocolic Omentum. Tissue Eng Part C Methods. 2016/06/19. 2016;22(8):740–6.
131. Traini T, Degidi M, Sammons R, Stanley P, Piattelli A. Histologic and elemental microanalytical study of anorganic bovine bone substitution following sinus floor augmentation in humans. J Periodontol. 2008/07/04. 2008;79(7):1232–40.
132. Shoulders MD, Raines RT. Collagen structure and stability. Annu Rev Biochem. 2009/04/07. 2009;78:929–58.
133. Somaiah C, Kumar A, Mawrie D, Sharma A, Patil SD, Bhattacharyya J, et al. Collagen Promotes Higher Adhesion, Survival and Proliferation of Mesenchymal Stem Cells. PLoS One. 2015/12/15. 2015;10(12):e0145068.
134. Rutkovskiy A, Stenslokken KO, Vaage IJ. Osteoblast Differentiation at a Glance. Med Sci Monit Basic Res. 2016/09/27. 2016;22:95–106.
135. Huang W, Yang S, Shao J, Li YP. Signaling and transcriptional regulation in osteoblast commitment and differentiation. Front Biosci. 2007/05/09. 2007;12:3068–92.

8. Publications

Comparison of different grafts and processing methods in relation to mesenchymal stem cell usage. Rasch A, Naujokat H, Wang F, Seekamp A, Klüter T, Fuchs S, (2018) Life Sciences Student Conference Kiel 2018, Kiel Germany, Poster

Rasch, A., Naujokat, H., Wang, F., Seekamp, A., Fuchs, S., & Klüter, T. (2019). Evaluation of bone allograft processing methods: Impact on decellularization efficacy, biocompatibility and mesenchymal stem cell functionality. *PloS one*, *14*(6), e0218404. https://doi.org/10.1371/journal.pone.0218404

Evaluation of bone allograft processing methods: Impact on decellularization efficacy, biocompatibility and mesenchymal stem cell functionality. Rasch A, Naujokat H, Wang F, Seekamp A, Klüter T, Fuchs S, (2019) European Orthopaedic Research Society, Annual Meeting EORS 2019, Maastricht Netherlands, Oral Presentation

Klüter, T., Hassan, R., Rasch, A., Naujokat, H., Wang, F., Behrendt, P., Lippross, S., Gerdesmeyer, L., Eglin, D., Seekamp, A., & Fuchs, S. (2020). An *Ex Vivo* Bone Defect Model to Evaluate Bone Substitutes and Associated Bone Regeneration Processes. *Tissue engineering. Part C, Methods*, *26*(1), 56–65. https://doi.org/10.1089/ten.TEC.2019.0274

I am thankful to Kieler Ärzteverein e.V. (Association of medical doctors in Kiel, Germany) for granting a travel scholarship for the purpose of visiting the Annual Meeting 2019 of the European Orthopaedic Research Society. On this occasion, “Evaluierung von Knochen-Allograft-Dezellularisationsmethoden zur Nutzung in Verbindung mit Mesenchymalen Stammzellen (MSCs)” was presented at the Annual Meeting of the Kieler Ärzteverein e.V.

9. List of Materials

9.1. Instruments

Instrument	Model	Manufacturer
Bandsaw	Metabo BAS	Metabo, Nürtingen, Germany
Beakers	DURAN	SCHOTT, Mitterteich, Germany
Bone holding forceps	Patellar forceps 185 mm	Aesculap, Tuttlingen, Germany
Caliper	Pocket Vernier Calliper	STEINLE, Ingelfingen, Germany
CASY	CASY TT	OLS, Bremen, Germany
Centrifuge	Biofuge primo R	Heraeus, Hanau, Germany
	Multifuge 3 S-R	Heraeus, Hanau, Germany
Confocal laser scanning microscopy	LSM 510 Meta	Zeiss, Oberkochen, Germany
Cryo 1°C Freezing Container	NALGENE® Mr. Frosty	Thermo Scientific, USA
Cryotank	Locator 4 plus	Thermo Scientific, Marietta OH, USA
Dremel drilling machine	Dremel 3000	Dremel, Mt. Prospect, USA
Epi-fluorescent microscope	EVOS FL Auto 2	Life Technologies, Grand Island, USA
Fluorescent Microplate reader	Spectra FLUORA plus	TECAN, Maennedorf, Switzerland
Fridge (4°C)	Profi line	LIEBEHERR, Austria
Freezer (-20°C)	Premium Nofrost	LIEBEHERR, Austria

	Comfort	
Freezer (-80°C)	HERA freeze	Heraeus, Hanau, Germany
Fumehood	Köttermann	Köttermann, Uetze, Germany
Graphpad Prism 7	Graphpad software	GraphPad Software, Inc., La Jolla, CA, USA
Grinding machine	DP-U4	Struers, Erkrath, Germany
High precision bandsaw	Exakt 312	Exakt, Norderstedt, Germany
High precision grinding machine	Exakt 400 CS	Exakt, Norderstedt, Germany
Incubator	BBD6220 & HERA cell 240	Thermo Scientific, Langenselbold, Germany
Laminar flow bench	HERA safe	Heraeus, Hanau, Germany
Light microscope	Axiovert 25	Zeiss, Oberkochen, Germany
Luer forceps	Luer	Aesculap, Tuttlingen, Germany
Microcentrifuge	3722L	Fisher Scientific
	220VAC	ROTH
Orbital shaker	Swip	Edmund Bühler, Germany
Pipette aid	Pipetus	HIRSCHMANN LABORGERÄTE
Roller mixer	SRT9	Stuart, Staffordshire, UK
Scanning electron microscope (SEM)	Philips XL 30 CP SEM	Philips, Amsterdam, Netherlands

Sonicator	MSE	MSE, London, UK
Sputter coater	SCD 005 Cool Sputter Coater	Bal-Tec, Balzers, Lichtenstein
Surgical kit	Surgical kit	Aesculap, Tuttlingen, Germany
Thermoblock	Thermomixer comfort	Eppendorf, Hamburg, Germany
Tissue Processor	Tissue Processor TPC 15	Medite, Burgdorf, Germany
Vaccum pump	AC500	HLC, Bovenden, Germany
Vaccum aid	Vacu boy	Integra Biosciences, Fernwald, Germany
Vortex	VORTEX-GENIE 2	Scientific Industries, Bohemia, NY, USA
Waterbath	1004	GFL, Burgwedel, Germany
Weighing machine	BP211D	Sartorius

9.2 Consumables

Consumables	Manufacturer
24-well-plates lid, sterile	TPP, Trasadingen, Switzerland
48-well-plates lid, sterile	Falcon, corning NY, USA
96-well-plates lid, sterile	Sarstedt, Nümbrecht, Germany
96-well-plates, F, Trans	Greiner bio-one, Frickenhausen, Germany
Aluminum foil	Universal, Düsseldorf, Germany
Carbon adhesive discs	Agar Scientific, Stansted, UK
Cell scrapers	Sarstedt, Nümbrecht, Germany
Cell Strainers 40 μm Nylon	Falcon, Durham, USA
Centrifuge Tubes (15mL, 50mL)	Sarstedt, Nümbrecht, Germany

Filter 0.2 μm non-pyrogenic	Sarstedt, Nümbrecht, Germany
Microtubes (500μL, 1.5mL, 2mL)	Sarstedt, Nümbrecht, Germany
Needles 20G×1 ½", Sterican®	B.BRAUN, Melsungen, Germany
Pasteur pipettes	Assistant, Germany
pH-indicator paper pH1-14	Merck, Darmstadt, Germany
Pipette tips (10, 200, 1000μL)	Sarstedt, Nümbrecht, Germany
Serological Pipettes (5mL, 12mL and 25mL)	Sarstedt, Nümbrecht, Germany
Specimen-tables	Agar Scientific, Stansted, UK
Sterile surgical gloves	CardinalHealth, Dublin, OH, USA
Syringe (5mL, 10mL, 20mL)	BD, Madrid, Spain
Tissue culture flasks vent. Cap (T25, T75, T175)	Sarstedt, Nümbrecht, Germany

9.3 Supplies

Name	Manufacturer
Alizarin Red S Stain Solution	Millipore, Billerica, USA
Accutase®	Biowest, Nuaillé, France
Ascorbic acid	Sigma-Aldrich, Darmstadt, Germany
2,2′-Azobis(2-methylpropionitrile)	Merck, Darmstadt, Germany
β-Glycerophosphate	Sigma-Aldrich, St. Louis, MO, USA
Bio-Oss®	Geistlich, Wolhusen, Switzerland
Biocidal	WAK Chemie Medical, Steinbach, Germany
Bovine serum albumin (BSA)	Millipore, Kankakee, USA
Calcein AM fluorescent dye	BD Biosciences, Bedford, USA
Cell Tracker	Invitrogen, Eugene, USA
Collagen type I (rat tail)	Corning, Bedford, MA, USA
Cetylpyridinium chloride (CPC)	Roth, Karlsruhe, Germany
Cyproby	FRESENIUS KABI, Bad Homburg, Germany

Dulbecco's Medium Essential Medium (DMEM)/Ham F-12 1:1	Biochrom, Berlin, Germany
Dexamethasone	Sigma-Aldrich, St. Louis, MO, USA
Dimethyl sulfoxide (DMSO)	Sigma-Aldrich, St. Louis, MO, USA
Ethylendiaminetetraacetat (EDTA)	SERVA, Heidelberg, Germany
Ethanol	Merck, Darmstadt, Germany
Fetal bovine serum (FBS)	Sigma, Taufkirchen, Germany
Fibronectin	Millipore, Temecula, CA, USA
Formic acid	Merck, Darmstadt, Germany
Fungizone	Biozol, Eching, Germany
Glutaraldehyde	Sigma-Aldrich, Darmstadt, Germany
Hexamethyldisilazane	ThermoFisher, Kandel, Germany
Hoechst	Sigma-Aldrich, Darmstadt, Germany
Isopropanol	Merck, Darmstadt, Germany
Medium 199 GlutaMAX™	Gibco, Darmstadt, Germany
Methanol	Carl Roth, Karlsruhe, Germany
Methyl methacrylate (MMA)	Fluka, Neu-Ulm, Germany
Nonylphenol-polyethylene glycol acetate	Walter-CMP, Kiel, Germany
Nuclease-free water	Ambion, Carlsbad, CA, USA
Paraformaldehyde solution in PBS 4%	Morphisto, Frankfurt am Main, Germany
Phalloidin-TRITC	Sigma-Aldrich, St. Louis, MO, USA
Penicillin/ streptomycin (Pen/Strep)	Biochrom, Berlin, Germany
Phosphate buffered saline (PBS) 10×	Gibco, Darmstadt, Germany
Phthalic acid butyl ester	Merck, Darmstadt, Germany
SDS	Sigma-Aldrich, St. Louis, MO, USA
Toluidine blue staining solution	Merck, Darmstadt, Germany
Triton® X-100	Sigma-Aldrich, Taufkirchen, Germany
Tutoplast®	RTI Surgical, Alachua, FL, USA

Water Ampuwa®	FRESENIUS KABI, Bad Homburg, Germany

9.4 Buffers and media

Buffer	Composition
Buffy-coat buffer	2mM EDTA, 0.5% (v/v) FBS in PBS
Tissue buffer	15% (v/v) FBS, 1% Pen/Strep, 1% Fungizone and 1% Cyproby in Medium 199 GlutaMAX™
MSC growth medium 10% FBS	10% (v/v) FBS, 1% Pen/Strep in DMEM/Ham's F-12 1:1
MSC growth medium 20% FBS	20% (v/v) FBS, 1% Pen/Strep in DMEM/Ham's F-12 1:1
Osteogenic differentiation medium (ODM)	10% (v/v) FBS, 1% (v/v) Pen/Strep, 10 mM β-glycerol phosphate, 0,1 µM dexamethasone and 50 µM ascorbic acid in DMEM/Ham's F-12 1:1

9.5 Kits

Kits	Manufacturer
Alkaline phosphatase assay kit	Abcam, Cambridge, UK
CellTiter 96® AQueous One Solution Cell Proliferation Assay	Promega, Madison, USA
Quant-iT PicoGreen dsDNA assay kit	Molecular probes, Oregon, USA

10. Acknowledgement

I thank Prof. Andreas Seekamp for the leadership of the orthopedic and trauma surgery department at the University Medical Center Schleswig-Holstein, Campus Kiel and for the opportunity to do research in his lab.

I am indebted to Prof. Sabine Fuchs (Director of the Dept. of Experimental Trauma Surgery, University Medical Center Schleswig-Holstein, Campus Kiel) for her supervision of the research work, and for her guidance and instructions. Her pursuit for the best in all things has helped me to challenge my own work and to improve on it.

I am grateful to Dr. Tim Klüter (Dept. of Orthopedic and Trauma Surgery, University Medical Center Schleswig-Holstein, Campus Kiel) for his supervision, constant help and motivation.

I am thankful to Dr. Hendrik Naujokat (Dept. of Oral and Maxillofacial Surgery, University Medical Center Schleswig-Holstein, Campus Kiel) for providing bone graft material and for the connection to the Dept. of Maxillofacial Surgery at the University Medical Center Schleswig-Holstein, Campus Kiel.

I thank Fanlu Wang (Dept. of Experimental Trauma Surgery, University Medical Center Schleswig-Holstein, Campus Kiel) for her support in the lab.

I thank Anne-Rose Nissen (Formerly Dept. of Experimental Trauma Surgery, University Medical Center Schleswig-Holstein, Campus Kiel) for her introduction into cell culturing techniques and for her help.

I am thankful to Frank Lehmann (Dept. of Prosthodontics, Propaedeutics and Dental Materials, University Medical Center Schleswig-Holstein, Campus Kiel) for his instruction and assistance with the scanning electron microscope.

I thank Gaby Neßenius (Dept. of Oral and Maxillofacial Surgery, University Medical Center Schleswig-Holstein, Campus Kiel) for her instruction and help in regard to histological hard grind slides.

I am especially thankful to Rywan Hassan (Dept. of Experimental Trauma Surgery, University Medical Center Schleswig-Holstein, Campus Kiel) for his introduction to working with human bone tissue and his constant motivation.

Finally, I want to thank the entire lab group for their support. Working in this group has been a blessing and has helped me to overcome challenges and obstacles on the way.

11. Declaration I

I hereby declare that I produced this work without the unauthorized help of third parties or any other aids, except when otherwise specified. The thoughts taken directly or indirectly from foreign sources are identified as such. This work has not yet been submitted to another examination authority either in Germany or abroad in the same or similar form.

Kiel, 24.06.2020

_____

Alexander Rasch

12. Declaration II

The present dissertation was prepared under the scientific supervision of Prof. Sabine Fuchs at the Department of Experimental Trauma Surgery of the University Medical Center Schleswig-Holstein, Campus Kiel, pertaining to Christian-Albrechts-University Kiel. Previous doctoral procedures did not take place.

Kiel, 24.06.2020

_____

Alexander Rasch